2013

Investigation of Microwave Technologies for Biochemical Applications

Valerie Terynn Tripp
College of William & Mary - Arts & Sciences

Investigation of Microwave Technologies for Biochemical Applications

Valerie Terynn Tripp

Littleton, Colorado

B.A. Chemistry, Macalester College, 2011

A Thesis presented to the Graduate Faculty
of the College of William and Mary in Candidacy for the Degree of
Master of Science

Chemistry Department

The College of William and Mary
August, 2013

COMPLIANCE PAGE

Research approved by

Institutional Biosafety Committee

Protocol number(s): IBC-2012-09-13-8113-DYOUNG01

Date(s) of approval: 09/13/2012

APPROVAL PAGE

This Thesis is submitted in partial fulfillment of
the requirements for the degree of

Master of Science

Valerie Terynn Tripp

Approved by the Committee, August, 2013

Committee Chair
Assistant Professor Douglas Young
College of William and Mary

Professor Deborah Bebout
College of William and Mary

Professor J.C. Poutsma
College of William and Mary

ABSTRACT

In recent years microwave irradiation has been exploited within synthetic chemistry to decrease reaction times while improving yields and purities for various organic reactions. This research set forth to investigate the application of microwave technology on the underutilized Glaser Hay reaction. We have developed solid supported reaction conditions by immobilizing one terminal alkyne on a polystyrene resin prior to coupling. The immobilization allows the reaction to progress with high levels of chemoselectivity, yielding the heterodimer polyyne. Typically such reactions can require 18-48 h of heating; however with the advantages afforded by the solid support, we reduced the reaction time to 16 h. This methodology not only decreased the reaction time of this reaction, but also helped to eliminate tedious separations and workups. The speed and efficiency of this method allowed for the production of a library of diverse polyynes for later screening. By transferring these reaction conditions to a microwave reactor, the coupling can be reduced to 10 min, however further optimization of the microwave-assisted coupling is still needed.

More recently microwaves have also been investigated with biological systems, including the activation of enzymes and the hybridization of DNA. Microwave irradiation is thought to induce molecular motion as the dipoles within a sample align with the oscillating electromagnetic field. Given the large dipole moments present within many biomacromolecules, these systems should be highly susceptible to microwave effects. To this effect, microwave irradiation was successfully employed as a method to introduce exogenous DNA into *E. coli*, with efficiencies of ~10^5 cfu. This is the first reported example of using focused microwave irradiation towards bacterial transformations. This technique demonstrates the potential of microwaves for further examination in biological systems.

TABLE OF CONTENTS

ACKNOWLEDGEMENTS

I would like to express my sincere thanks to Dr. Douglas Young for welcoming me into his lab and advising me for the last 2 years. It was an honor to have been his first student. I am grateful to my committee members, Dr. Bebout and Dr. Poutsma, for dedicating their time and energy to assist me with my thesis. Much of my work would not have been possible without the help of several other labs including the Harbron Lab, the Poutsma Lab, and the Scheerer Lab. I would also like to acknowledge the Chemistry Department at College of William and Mary for instructing and guiding me for the past 2 years. To my fellow Young Lab members, I sincerely thank you for all that you have taught me and for granting me the privilege to teach you. For those who stayed during the 2013 summer, Ben, Chris, Corinn, Jackie, Johnathan, and Ryan, I am incredibly thankful for the patience, encouragement, and entertainment you offered during this chaotic time. I would like to acknowledge the other chemistry graduate students, especially Will Czaplyski and Kaila Margrey. Kaila, you inspire me with your passion and tenacity for all things. Will, you always manage to brighten my day and I am constantly amazed by your humility and kindness. I am a better person and chemist for meeting you two. I would like to thank Daniel Ressler for all of his help, support, and most of all his patience. Finally, thanks to my family, Tripps, Frybergers, and Resslers, your love drives me to follow my dreams, wherever they may lead.

For Nana

LIST OF FIGURES

LIST OF SCHEMES

LIST OF TABLES

Chapter 1: Introduction to Microwave Irradiation

1.1. Historical Perspectives on Microwave Irradiation

Though microwaves have long been known for their application in the heating of materials, it was not until 1986 that they were found to enhance organic reactions compared to conventional thermal convection methods.[1,2] However, the lack of control and reproducibility of the microwave field hindered the advancement of the field. Moreover, microwave-assisted reactions also are associated with safety risks when flammable organic solvents are exposed to a microwave field without proper temperature and pressure controls. Given these limitations, microwave technology has developed rather slowly, but technological advances from modified kitchen microwaves to instruments specifically designed for chemical synthesis have facilitated its evolution.

The utilization of microwave irradiation in organic synthesis has increased product yields while reducing reaction times compared to conventional heating methods. Due to these advantages, microwave assisted reactions have gained increased use, including application in medicinal chemistry, peptide synthesis, material sciences, and polymer synthesis.[3,4,5,6]

1.1.2 Theory of Microwave Irradiation

Microwaves typically have wavelengths ranging from 1 mm to 1 m with frequencies of 0.3 to 300 GHz, placing them between infrared radiation and radio waves within the electromagnetic spectrum (Figure 1.1).[7]

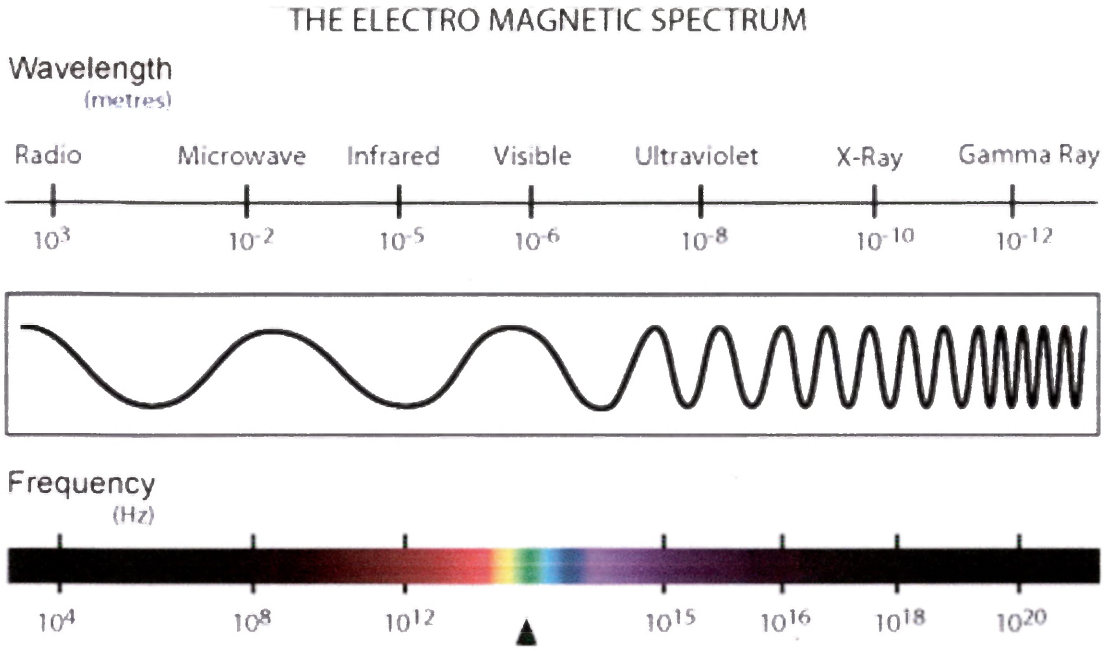

Figure 1.1 – The wavelengths and frequencies of the electromagnetic spectrum.[7]

The two components of a microwave, an electric field and a magnetic field, are hypothesized to efficiently heat various materials through a phenomenon known as "microwave dielectric heating".[8]

The electric portion of the field generates heat through dipolar polarization and conduction. During irradiation with microwaves, dipoles or ions align with the applied electric field by rotating. As the electric field oscillates, the dipole or ion attempts to realign with the varying field, losing energy as heat through molecular friction (Figure 1.2).[9]

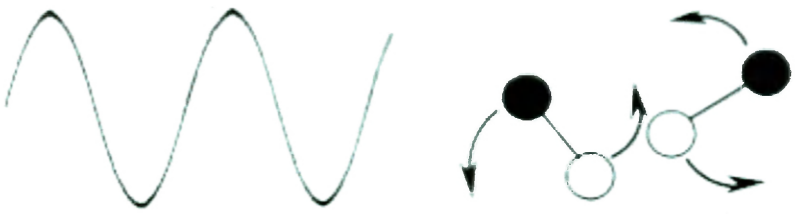

Figure 1.2 – Molecules that possess a dipole re-orient in order to align with the alternating electric field from the microwave irradiation.[9]

However, the frequencies within the microwave region are low enough that the dipoles do not have sufficient time to respond to the varying electric field. Thus as the dipole re-arranges, the electric field is already alternating, causing a phase difference between the orientation of the dipole and the electric field. As a result, energy is lost from the dipole by molecular collisions and friction, leading to dielectric heating.[10,11]

The response of a specific solvent to microwave irradiation largely depends the ability of its dipole to interact with the electromagnetic field. Thus, common organic solvents are often categorized by their microwave-absorbing properties, high, medium, or low.[12] Certain solvents that lack a permanent dipole moment, such as benzene, are more or less transparent to the microwave irradiation. These transparent solvents are often advantageous for use with chemical reactions, since they allow the microwave energy to directly interact with the dipole moments present within the reagents.

While conventional heating apparatuses, like oil baths and sand baths, transfer heat to reactions, they are often inefficient; generating a temperature gradient within a sample due to poor heat transfer. Typically, the reaction mixture in contact with the walls of the vessel heats most rapidly, however such localized overheating can cause decomposition of reagents, substrates, and products. Conversely, microwave irradiation interacts directly

with the sample, obviating the establishment of a temperature gradient, and heating the reaction more efficiently (Figure 1.3).[9]

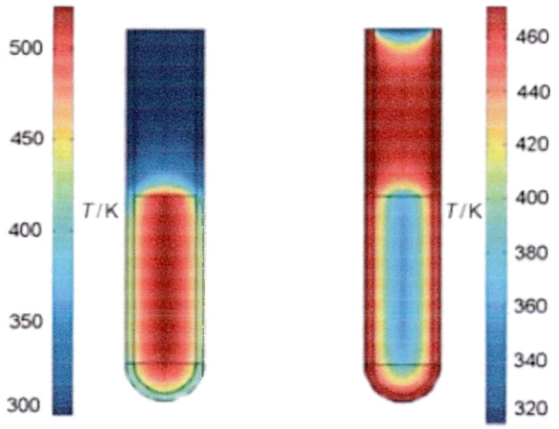

Figure 1.3 – Comparison of temperature profiles for microwave (left) compared to oil bath heating (right). The sample exposed to microwave irradiation experiences bulk heating of the solvent, while the oil bath heats the vessel first.[9]

Since the microwave reaction vessels are made out of microwave-transparent materials, such as quartz or borosilicate glass, the irradiation efficiently heats the reaction directly rather than the vessel.[10] The direct irradiation from the reactor results in bulk heating of the sample, increasing the temperature of the entire volume uniformly and rapidly.

1.1.3 Applications in Chemical Synthesis

The shorter reaction times achieved with microwave irradiation represents a desirable tool to allow for the rapid production and biological screening of various molecules. Additionally, the use of microwave technologies towards organic syntheses has resulted in fewer side reactions, increased yields, and improved reproducibility. Due

to the substantial benefits provided by microwave irradiation, many studies have focused on further developing this cutting-edge technology. To date, microwave-assisted organic synthesis has included optimizing reaction conditions, synthesizing new chemical structures, and investigating chemical reactivities.

One of the most studied and characterized subset of microwave reactions includes reactions with homogenous transition-metal catalysts, forming carbon-carbon or carbon-heteroatom bonds.[12] Traditionally, these bond-forming reactions are heated to reflux under an inert atmosphere, often requiring hours or days to achieve completion. Conversely, enhanced rates have been observed for many of these couplings through the utilization of microwave heating in sealed vessels. Moreover, the reactions can often progress without the need for an inert atmosphere. Previous reports hypothesize that transition metal-based catalysts interact directly with the microwave irradiation, leading to the acceleration of reactions.[11] Furthermore, catalysts used in microwave-assisted reactions displayed increased lifetimes due to the uniform temperature profile.

Microwave-assisted syntheses have been reported for the major carbon-carbon bond forming reactions including Heck, Suzuki, and Sonogashira couplings.[12] Literature precedent also exists for utilizing microwave technology as a convenient tool to form carbon-heteroatom bonds, to cyclize various compounds, and to deprotect multiple functional groups.[13,14,15] We aim to investigate the application of microwave technology on the underutilized Glaser Hay reaction. Ideally, the development of a microwave-assisted methodology for this reaction would drastically decrease reaction times while improving overall yields.

Chapter 2: Solid Supported Glaser Hay Coupling Reactions

2.1 Introduction to Glaser Hay Coupling

2.1.1 Polyyne Structures – Applications and Synthetic Approaches

Acetylenic scaffolds, or diynes, are observed as core structures in various natural products, many polymers, and other supramolecular materials (Figure 2.1).[16] To date, over one thousand naturally occurring polyynes have been isolated and found to exhibit a range of biological activities; including antifungal, anticancer, anti-HIV, and antibacterial properties.[5] Within polymer structures, acetylenic cores provide a versatile linear structural moiety giving rise to unique optical properties. For example, when coupled with transition metals, these organometallic materials display various novel properties, such as luminescence, conductivity, and photovoltaic behavior.[17]

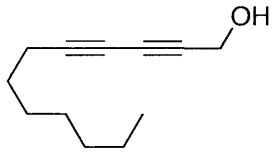

Montoporic Acid A

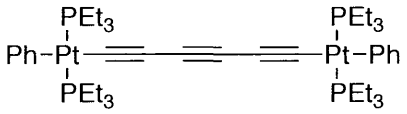

Platinum triacetylenic polymer

Figure 2.1 – Various acetylenic core structures. Montoporic acid is a natural product produced by a velvet coral that has been shown to exhibit antifungal and antibacterial properties. Platinum triacetylenic polymer possesses unique optic and luminescecent qualities.

Glaser first described the synthesis of the unique polyyne core structure in 1869, after the oxidative dimerization of copper (I) phenylacetylide upon exposure to air (Scheme 2.1). The applications of the original synthesis were initially limited by the

required isolation of the reactive copper acetylide prior to oxidation. Further investigations revealed the potential of forming the species *in situ*, thereby improving the convenience and range of the coupling reaction, specifically in industrial settings.

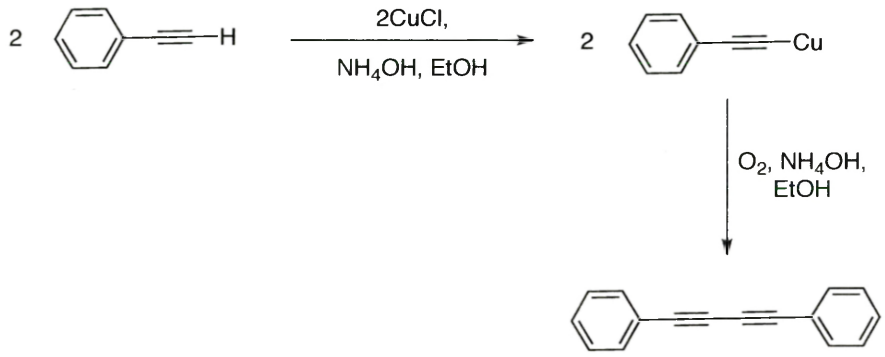

Scheme 2.1– The first polyyne synthesis reported by Glaser.

2.1.2 Mechanistic Studies of Copper-Mediated Acetylenic Couplings

While several coupling variations have been observed and reviewed since Glaser's initial discovery, the mechanism for this reaction has not been fully elucidated though several hypotheses currently exist. Perhaps one of the earliest mechanistic studies proposed the formation of radical species that combined to yield the subsequent diyne. Kinetic investigations of the Glaser coupling conditions revealed the role of the copper (II) ions as the direct oxidizing agent. Furthermore, the rate of the coupling reactions increased in situations with more acidic terminal alkynes and a more alkaline solvent environment.[18] From these observations, Klebansky et al. suggested that the reaction proceeded through the heterolytic cleavage of the terminal proton to give an anionic

intermediate. Next, the acetylenic anion transferred a single electron to the copper (II) salt, generating the terminal radical for further reaction (Scheme 2.2).

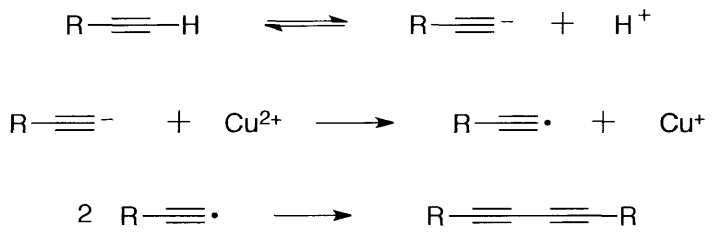

Scheme 2.2 –Proposed radical mechanism for the oxidative homocoupling of two terminal alkynes.

A breakthrough report from Bohlmann et al. in 1964 reinforced the kinetic trends observed with acidic alkynes and basic environments. Yet, under acidic reaction conditions (pH 3), the rate of dimer formation decreased for acidic alkynes necessitating the addition of more copper (I) salt.[19] Given this additional information, Bohlmann proposed the creation of π complexes between the copper (I) ions and the triple bond of the alkyne, thereby activating the alkyne toward deprotonation.[20] As expected, the complexation would be weaker for conjugated alkyne systems, due to the diffused π systems, resulting in slower reaction rates. Results from the same study disputed the theory of free radical formation during the coupling mechanism. Reactions with electronically different alkynes primarily formed the symmetric coupling product rather than the asymmetric heterocoupling product. Such selectively would not be expected nor justified with radical intermediates. Consequently, Bohlmann suggested a dinuclear copper (II) complex that would collapse to directly form the coupled product (Scheme 2.3).[5]

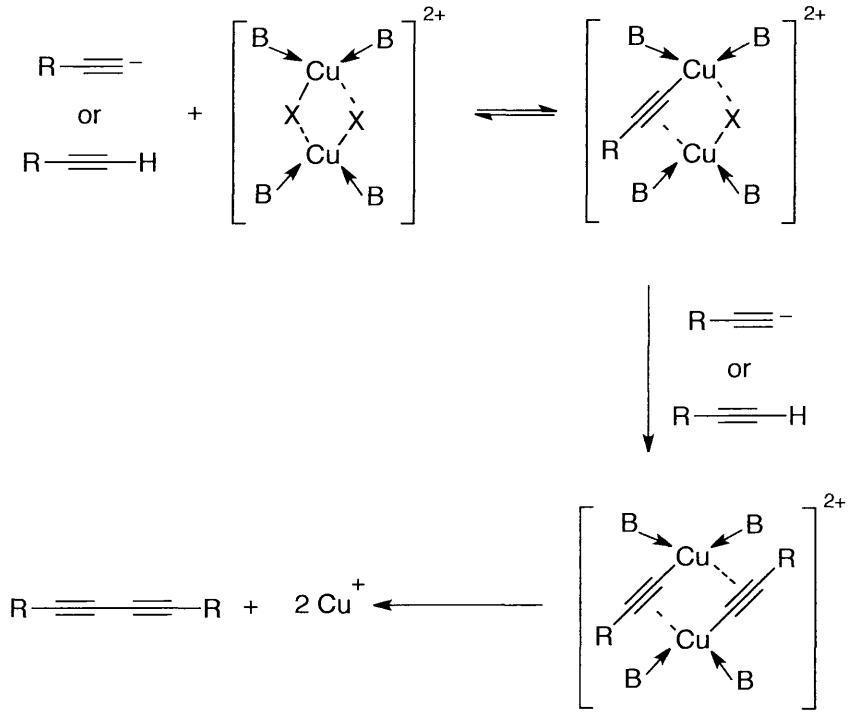

Scheme 2.3 – Bohlmann's proposed dinuclear copper (II) complex. B represents the appropriate ligand, such as TMEDA, X represents the country anion such as Cl^-.

Experimental observations supported this dimeric proposal, with the coupling rate kinetics being second order with respect to the alkyne concentration. Most of the subsequent mechanistic studies included this dicopper intermediate, however the details of the formation as well as the collapse of the complex tend to vary.

2.1.3 Expansions and Improvements to Glaser-type Couplings

Though classical Glaser coupling conditions are still principally utilized for homocoupling reactions, various modifications and enhancements have been developed

to decrease reaction times while improving yields. Several approaches focused on the optimization of various conditions within the reaction, including the copper salt, solvent, temperature, time, and oxidizing agents, in order to promote more effective alkyne-alkyne coupling. One method, described by Hay, requires dissolving catalytic amounts of copper (I) chloride in the presence of the bidentate tetramethylenediamine (TMEDA) and oxygen; forming the reactive intermediate *in situ*, and thereby drastically decreasing the reaction time (Scheme 2.4).[21] Known as the Glaser Hay coupling, this variant provides an efficient procedure for generating symmetric diyne compounds in relatively high yields.

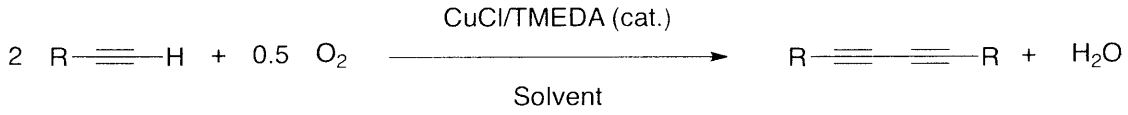

Scheme 2.4 – Standard Glaser Hay reaction conditions.

However, one major drawback of these reaction conditions is the lack of chemoselectivity with regards to asymmetric coupling. When two electronically different terminal alkynes are coupled by a Glaser Hay reaction, three potential polyyne compounds are generated (Scheme 2.5). As a result, further purification steps are required in order to isolate the desired asymmetric dimer.

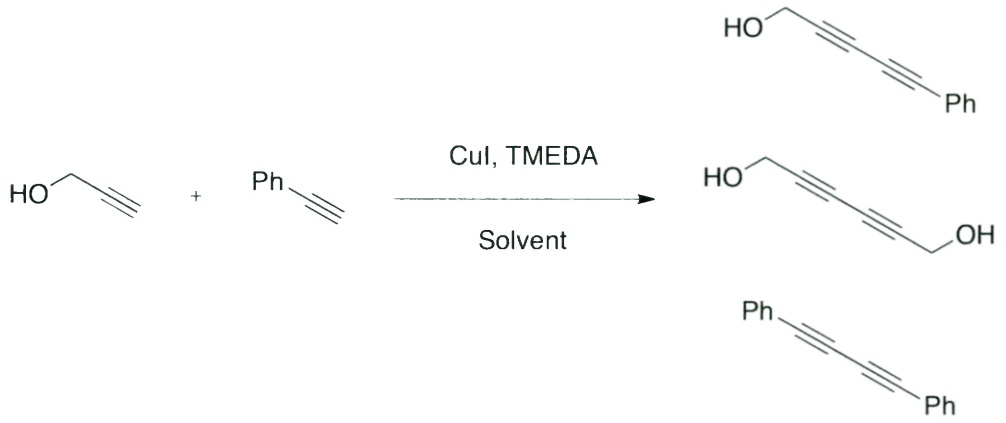

Scheme 2.5 – Under standard Glaser Hay conditions, three polyyne products are formed.

In order to overcome the issue of selectivity, Chodkiewicz and Cadiot reported an improved protocol towards the non-symmetric coupling of a terminal alkyne with 1-bromacetylene partners (Scheme 2.6).[22] This method is particularly effective with terminal alkynes containing a hydrophilic moiety, such as a carboxylate or amine, or a conjugated system. While bromo-alkynes and iodo-alkynes have been successfully employed for Cadiot-Chodkiewicz coupling reactions, chloro-acetylenes remain impractical due to their limited reactivity.

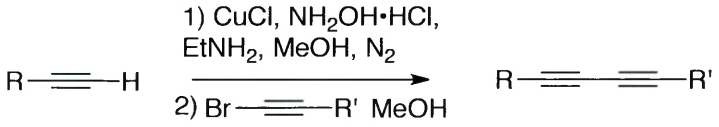

Scheme 2.6 – Conditions for standard Cadiot-Chodkiewicz coupling towards the formation of asymmetric polyynes.

Initially the haloalkynes were observed to undergo a self-coupling side reaction to yield symmetrical polyacetylenes.[15] Incorporating amines into the reaction and lowering the concentration of haloalkyne prevents the formation of the undesired homodimer. The

improved chemoselectivity of this method has been effectively utilized to synthesize a wide range of molecules with diverse chemical functionalities. Though several variations have been developed, the original Cadiot-Chodkiewicz reaction conditions serve as the main route for the synthesis of non-symmetric diynes. The heterocoupling was employed to successfully construct countless carbon frameworks, including the polyyne core of panaxydol, an antitumor agent originally isolated from the *Panax ginseng* plant (Scheme 2.7).[23]

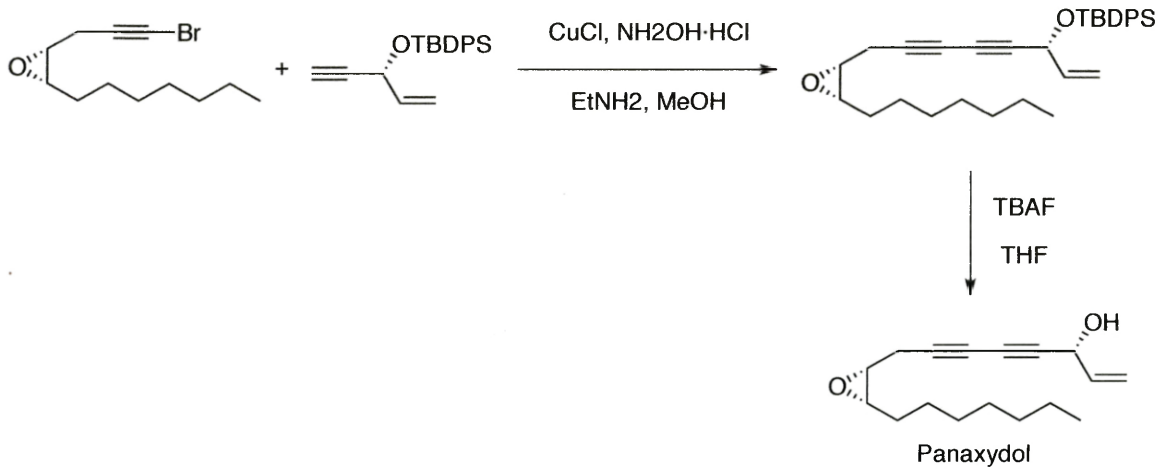

Scheme 2.7 – Cadiot-Chodkiewicz reaction to prepare the carbon frame of the natural product panaxydol.

2.1.4 Current Limitations with Coupling Reactions

Glaser, Hay, and Cadiot-Chodkiewicz coupling conditions, as well as their respective variants, offer effective pathways to form extremely diverse compounds with polyyne functionalities. Though there are multiple advantages for each synthetic pathway, there are also distinct limitations. The original Glaser coupling and the Hay modification both

lack chemoselectivity in the generation of asymmetric diynes. As a result, more thorough purification techniques are necessary before isolating the desired heterocoupled product. The inherent side reactions result in lower yields as some of the starting material is consumed to form the homodimer. Furthermore, the Glaser and Hay methodologies typically require several hours of stirring at room temperature in order to yield desired product. Depending on the specific reactants, the coupling process can range from 3hr-48 hr. While the Cadiot-Chodkiewicz variation overcomes the issue of chemoselectivity, the reaction requires the preparation of a halo-alkyne, rather than two terminal asymmetric alkynes, and does not completely eliminate the possibility of homocoupling. Additionally, the reaction times for the Cadiot-Chodkiewicz still extend from 0.5-12 hr based on the reaction components.

2.1.5 Advantages of Solid Support Organic Synthesis

To specifically address the problem of chemoselectivity for heterocouplings, one of the terminal alkynes can be immobilized on a polystyrene solid support. After immobilization, the standard Glaser Hay conditions can be utilized with higher levels of chemoselectivity, yielding a specific heterodimer. Furthermore, the incorporation of a solid support eliminates the need for tedious separations and workups.

Originally developed for the synthesis of peptides, solid supports have been increasingly utilized in organic synthesis. The insoluble polymeric backbone provides a unique surface for synthetic transformations, allowing the products to be isolated from the solution phase by attachment to the resin. This aspect of solid support reactions

facilitates separation and purification by simple filtration and washing of the resin. Any unbound impurities or unreacted material is dissolved then washed away by rinsing the resin in a variety of solvents. Additionally, solid supports allow excesses of solution phase reagents since any unreacted reagents will also be removed during the filtration and washing process. Therefore, reactions can be driven to completion, yielding more product than the same reactions conducted in the solution phase.

Due to the ease of automization and ability to conduct parallel reactions, solid-phase organic synthesis provides an effective method for producing combinatorial libraries, especially in pharmaceutical settings. The ultimate aim of combinatorial synthesis is to simultaneously produce several different compounds with a common structural motif. To this end, various chemical building blocks are systematically assembled in multiple combinations to yield a large set of diverse molecules. Solid supports offer an ideal tool for the development of such libraries given the physical linkage of the product to the resin and the ability to rinse away unbound reactants.

2.1.6 Literature Review of Solid Support Applications

Given the unique advantages that solid supports provide, they have been used extensively for a variety of organic syntheses. . One such example utilized a polystyrene based solid support in combination the well-known Cadiot-Chodkiewicz heterocoupling conditions. Due to the loading capabilities of solid supports, the immobilized starting material exists in relatively small concentrations. The rigidity and dilute environment offered by the solid support eliminated the self-coupling that was typically observed with the corresponding solution phase Cadiot-Chodkiewicz reactions. By immobilizing the

haloalkyne partner, the reaction proceeded in higher yield without the generation of undesired homocoupled products (Scheme 2.8).

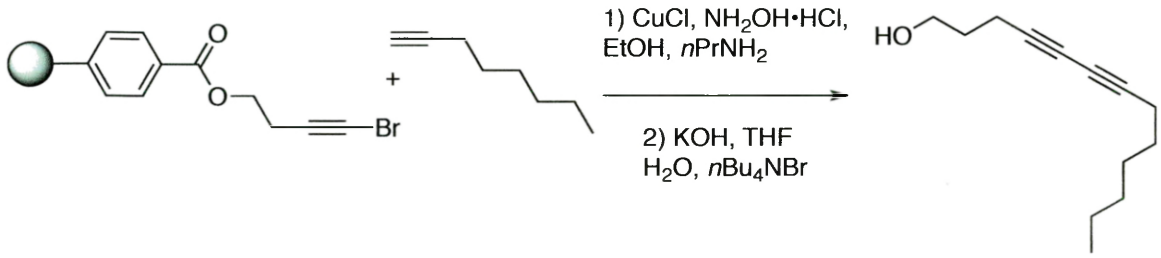

Scheme 2.8 – Merrified resin-assisted Cadiot-Chodkiewicz heterocoupling.

To generate an entire library of asymmetric diynes, the coupling reactions occurred under inert atmosphere and proceeded for 2 d. After simple filtration of the resin, washing, and cleavage, only trace amounts of homo-coupled product were observed, while the similar reactions conducted in solution phase produced about 34% homocoupled side products.

Sonogashira couplings present another application of solid phase organic synthesis, specifically in the formation of chemoselective products or complex ring systems. For instance, iodoanilines were immobilized on a polystyrene resin by a Rink amide linkage (Scheme 2.9).[24] The aryl iodides were then cross-coupled with terminal acetylenes in the presence of copper and palladium catalysts.

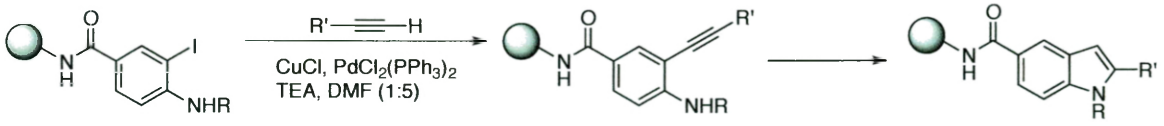

Scheme 2.9 – Polymer-assisted synthesis of substituted indoles utilizing Sonogashira coupling.

With the unsubstituted aniline starting material, the alkyne product was isolated in a 96% yield after 16 hr at 80 °C. Substituted anilines underwent further cyclization on the resin to produce the corresponding substituted indoles in yields above 86%. Though exploiting the resin improved the yields of the synthesis, the reactions remained limited by long reaction times of 16-24 h and large amounts of catalytic materials.

The combination of these solid support reaction conditions with microwave technologies was investigated in order to decrease the reaction times. In comparison, the microwave-assisted coupling of aryl iodide and various terminal alkynes achieved full conversion after only 15 min. After the aryl iodide was immobilized to a polystyrene support with a Rink amide linker, the coupling reactions were conducted with standard Sonogashira catalysts and additives. The mixture of derivatized resin and catalysts were irradiated in a single-mode microwave to reach a temperature of 120 °C. The use of microwave technology in concert with solid-phase organic synthesis resulted in yields of 89%-98% for the coupled products. This method allows for the rapid and efficient synthesis of acetylene derivatives through Sonogashira coupling. Similar microwave-assisted solid phase organic syntheses have been reported for Suzuki, Stille, and Heck reactions.[25, 26, 27] The incorporation of the microwave technology with the resin immobilization shortens the reaction time and provides an ideal method for the rapid generation of combinatorial libraries.

2.2 Solid-Supported Glaser Hay Couplings

2.2.1 Development of Reaction Conditions

Due to chemoselectivity issues associated with the Glaser Hay coupling, we selected this reaction as a model to apply the advantages of solid-supported chemistry. The resin can be derivatized to possess a terminal alkyne functionality that can be employed in coupling reactions. Three specific alkynes (**1-3**) were selected for immobilization on the resin and additional alkynes (**1-10**) were utilized as coupling partners (Figure 2.2). The coupling reactions were conducted on a diverse selection of alkynes in order to assess the versatility of the solid-phase methodology.

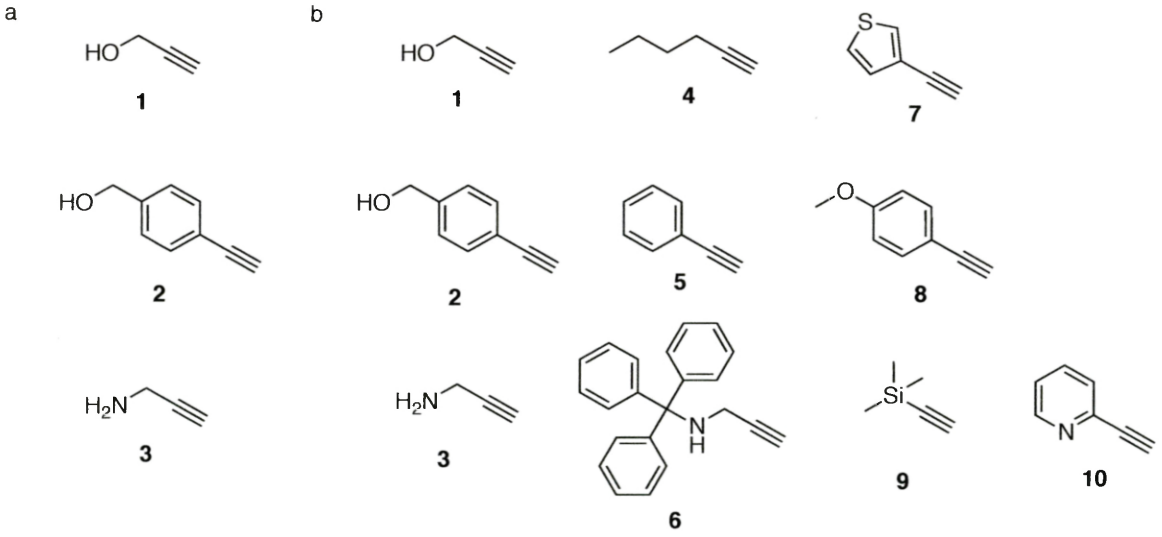

Figure 2.2 – (a) Alkynes selected for immobilization on the solid-support and (b) alkynes employed for coupling reactions.

The three alkynes were immobilized on a trityl chloride modified polystyrene resin (100-200 mesh) with 1% cross-linked divinylbenzene. The trityl linker can easily be cleaved under mildly acidic conditions and can afford coupled diyne products with the

highest purity. Initially substrate **1**, propargyl alcohol, was immobilized onto the solid support under standard conditions at room temperature (Scheme 2.10).

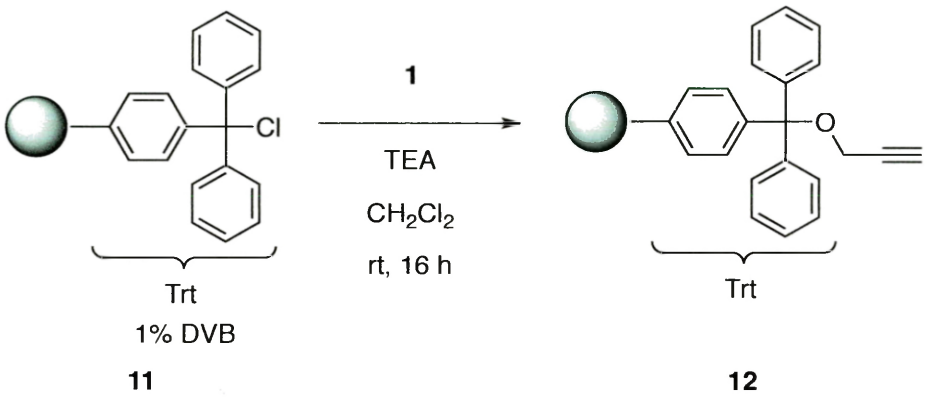

Scheme 2.10 – Attachment of substrate to 1% cross-linked polystyrene resin.

The coupling reaction conditions were initially optimized using the alcohol-derivatized resin **12** and phenylacetylene **5**. This specific coupling could be easily monitored with both thin layer chromatography and proton NMR spectroscopy. The immobilized propargyl alcohol **12** was treated with the solution phase alkyne (50 equiv.) in the presence of a copper/TMEDA catalyst at 25 °C for 16 hours (Scheme 2.11).

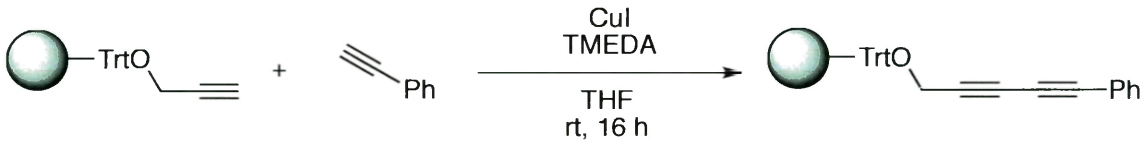

12 **5** **13**

Scheme 2.11 – Generic reaction for solid phase-supported Glaser Hay coupling at room temperature.

The coupled product was cleaved from the resin by treatment with 2% trifluoroacetic acid, TFA, in CH_2Cl_2 for 1 hour. Once the solution was filtered and the solvent was removed

in vacuo, the sample was analyzed by TLC and ^{1}H NMR (Scheme 2.12).

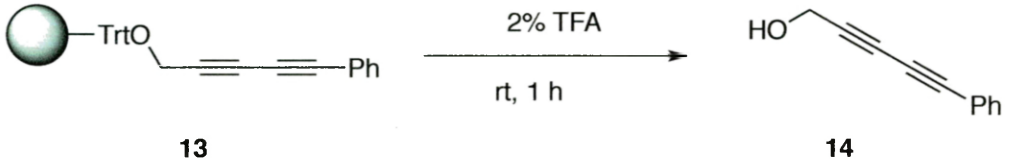

13 **14**

Scheme 2.12 – A generic cleavage reaction from the trityl linker of the resin to yield the polyyne product.

The hydrophobic polystyrene core allows the resin to swell in the presence of non-polar solvents; however, this property also ensures that the resin contracts when exposed to polar solvents. To this end, various reaction solvents were investigated including toluene, THF, CH_2Cl_2, and acetonitrile. Ideally, we hypothesized that a more non-polar solvent would expand the resin, making its reactive sites more accessible for the coupling reaction. While the resin expanded most visibly in the relatively non-polar CH_2Cl_2, THF was found to provide the ideal environment for the reaction. The reactions conducted in THF consistently generated the highest yields for the formation of **17**, the desired diyne.

Multiple copper sources and catalyst systems were also examined for use with the solid-support coupling reactions including copper chloride (5 equiv.) and tetramethylethylenediamine (TMEDA; 5 equiv). When this copper source was employed for the coupling reactions, no discernable product was formed, indicating either a solubility or reactivity issue. Based on the successful coupling reported by Li et al., we explored the utilization of a copper iodide (0.5 equiv.) with *N,N*-diisopropylethylamine (1 equiv.) and *N*-bromosuccinimide (0.5 equiv.) system.[28] However, the reactions conducted with this catalyst only yielded trace amounts of product, possibly due to a negative

interaction with the polystyrene resin. Ultimately, copper iodide copper was selected with an accompanying TMEDA ligand in order to improve the solubility of the metal. A variety of copper concentrations were examined with this catalyst system. Initially, we anticipated that a large excess of copper (~5 equiv.) could be utilized to force the coupling reaction to completion. Additionally, due to the nature of the solid supported reactions, any unreacted copper would be removed during the wash cycles of CH_2Cl_2 and methanol. Immediately after the formation the catalyst was added to the resin reaction in one portion.

When reacted under the optimized conditions, the product was isolated in good yield as confirmed by ^1H NMR; however, incomplete conversion of propargyl alcohol starting material was detected. Upon further investigation, it was also found that there was dimerization of the immobilized alkyne, to give an undesired homodimer product. This dimerization issue was most prominent in reactions involving the propargyl alcohol-derivatized resin. The occurrence of the starting material and homodimer are especially unfortunate, negatively impacting the yield and requiring further purification steps. This is especially problematic as the employment of the solid support in these coupling reactions was intended to eliminate both of these issues. We sought to further optimize the reaction conditions to successfully drive the reaction to completion, but without producing the impurities.

In an effort to force the reaction to completion, we increased the temperature of the reaction mixture. Utilizing a hot oil bath, we continuously heated the coupling reactions at a specific temperature for 16 h. A range of temperatures was examined, including 30 °C, 60 °C, and 80 °C, with the 60 °C conditions yielding the most promising results. The

reactions at 30 °C still displayed signs of starting material, indicating that the temperature was not sufficient to force the reaction to completion. Meanwhile, the reactions stirred at 80 °C demonstrated complete conversion, but afforded lower yields. This noticeable decrease in the formation of diyne product most likely results from the overheating and destruction of some of the polystyrene resin. Some of the copper catalyst was also found to melt onto the walls of the reaction vessel during this trial, suggesting that the temperature may inactivate the catalyst, thereby reducing the efficiency of the reaction. Given this information, we proceeded with a 60 °C reaction temperature that effectively forced the reaction to completion, eliminating the appearance of propargyl alcohol **1** starting material. Unfortunately, this modification did not suppress the formation of propargyl alcohol homodimer during the course of the reaction.

2.2.2 Attempts to Suppress Homodimer Formation

We proposed that decreasing the initial loading of the solid support would efficiently prevent the undesirable dimerization of propargyl alcohol on the functionalized resin. Our initial preparation of the propargyl alcohol consisted of swelling the resin in CH_2Cl_2 for 15 min, followed by the addition of propargyl alcohol **1** (10 equiv.) and triethylamine (10 equiv.). The reaction was stirred for 16 h at room temperature in order to achieve maximum loading of the starting material. After the discovery of the cross-linked homodimer product, we attempted to generate lower loaded resins by decreasing the amount of reagents used in the immobilization step.

Employing the same trityl chloride resin, **11**, we used 10 equiv. of propargyl alcohol in the presence of 10 equiv. of triethylamine. The reaction was then stirred at 40

°C for 16 h, with the aim of achieving a higher loaded resin, ~1.0 mmol/g. An identical reaction was set up but heated to 40 °C for only 2 h in order to generate a medium loaded resin, ~0.6 mmol/g. After a sufficient work up, each version of the loaded resin was subjected to a coupling reaction with **5**; stirring at room temperature for 16 h followed by cleavage in 2% TFA (Scheme 2.13).

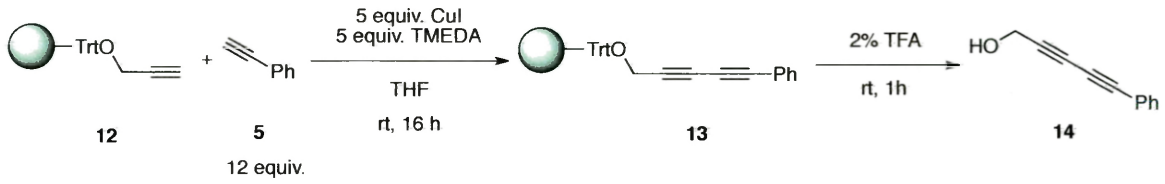

Scheme 2.13 – Coupling reaction and work up to yield desired diyne product **14**.

Analyzing both resin reactions by ^{1}H NMR revealed significant amounts of desired product **14** as well as homodimer impurity. While both samples contained the alcohol homodimer, the medium loaded resin, 0.6 mmol/g, contained 30% less than the high loaded reaction, 1.0 mmol/g, further confirming that the degree of loading dictates the formation of homodimer impurity. To combat the formation of the homodimer, several other equivalencies of propargyl alcohol were tested for loading onto the resin with varying degrees of success. Ultimately, even a trityl resin immobilized with only 1.2 equiv. of propargyl alcohol yielded homodimer, prompting us to utilize a more rigid polystyrene solid support. A 2-chlorotrityl chloride resin, 200-400 mesh, with 2% DVB crosslinking was selected for further immobilizations since the increased rigidity would prohibit the ability of resin bound alkynes to form crosslinked products. With such limited flexibility, two propargyl alcohol alkynes bonded to the same resin bead, would

not be able to physically bond to one another. A separate 2-chlorotrityl chloride resin, 200-400 mesh, with only 1% DVB crosslinking was also chosen for further analysis.

In order to better ascertain the concentration of propargyl alcohol **1** loaded during the immobilization process, samples of derivatized resin **12** were cleaved then directly analyzed by gas chromatography. Unfortunately, the presence of the 2% TFA significantly reduced the area of the peaks observed during the production of a calibration curve. Multiple standards of propargyl alcohol dissolved in only CH_2Cl_2 gave significantly larger peaks than the identical standards when dissolved in a 2% TFA solution. The dilute nature of the resin samples, compounded with the effects of the TFA made it difficult to accurately determine the concentration of propargyl alcohol. In an effort to remove the TFA from the samples, resin samples were cleaved and all solvent was removed *in vacuo*. During this process the TFA was also removed, leaving just the propargyl alcohol **1** from the resin. Unfortunately, when these samples were re-dissolved in CH_2Cl_2 and resubjected to GC analysis the resulting peaks were still insufficient to determine accurate concentrations of propargyl alcohol.

As an alternative, another set of resin samples were cleaved and the solvent was again removed *in vacuo*. The mass of the resulting product **1** was recorded and utilized to determine the relative loading of each resin in mmol substrate/g of resin. Through this method we calculated that the more rigid 2% cross-linked resin was loaded with 0.6 mmol/g to 0.7 mmol/g, while the 1% cross-linked resin was higher loaded with 1.5 mmol/g to 2.0 mmol/g. Based on this information, a series of coupling reactions were set up with the new 2-chlorotrityl resin types (Scheme 2.14).

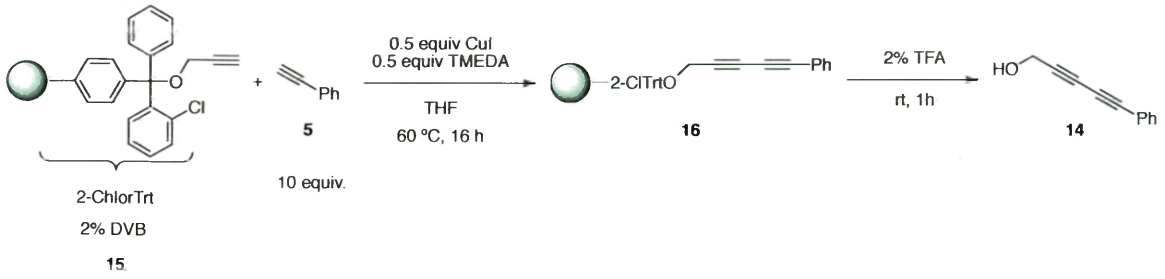

Scheme 2.14 – Coupling reaction with 2-chlorotrityl derivatized resin and phenylacetylene. Subsequent work up yielded the desired polyyne **14**.

The level of cross-linked DVB within the resin, usually 1% or 2%, showed little effect on the suppression of homodimer. This indicates that the concentration of loading plays a larger role in the formation of homodimer.After the necessary work up conditions, it was established that resin loaded above 0.7 mmol/g of propargyl alcohol forms undesired homodimer during the reaction conditions. Resin loaded at a concentration less than 0.7 mmol/g successfully eliminates homodimer formation while still generating sufficient amounts of diyne products.

2.2.3 Preparation of Diyne Library

In order to prepare a diverse library of diyne products, various alkynes were immobilized on the trityl chloride resin then submitted to optimized Glaser Hay reaction conditions. To fully access all possible reaction sites, the resin was incubated with THF and the soluble alkyne for 15 min prior to the addition of the catalyst mixture. After 16 h of stirring at 60 °C, the resin reaction was filtered then washed with alternating volumes of CH_2Cl_2 and methanol in order to remove unreacted reagents and other impurities. The resin was then cleaved with 2% TFA, the solvent was removed *in vacuo*, and the product was analyzed by TLC and ^{1}H NMR.

The 2-chlorotrityl resin was loaded with propargyl alcohol **1** at a level of 0.7 mmol/g of then employed in multiple coupling reactions under the previously optimized conditions. In order to remove any undesired homodimer from the product, the samples were cleaved in 2% TFA, filtered, then flushed through a silica plug. Any remaining solvent was removed *in vacuo* then each sample was analyzed by ^{1}H NMR, generating an entire library of diyne molecules (Table 2.1).

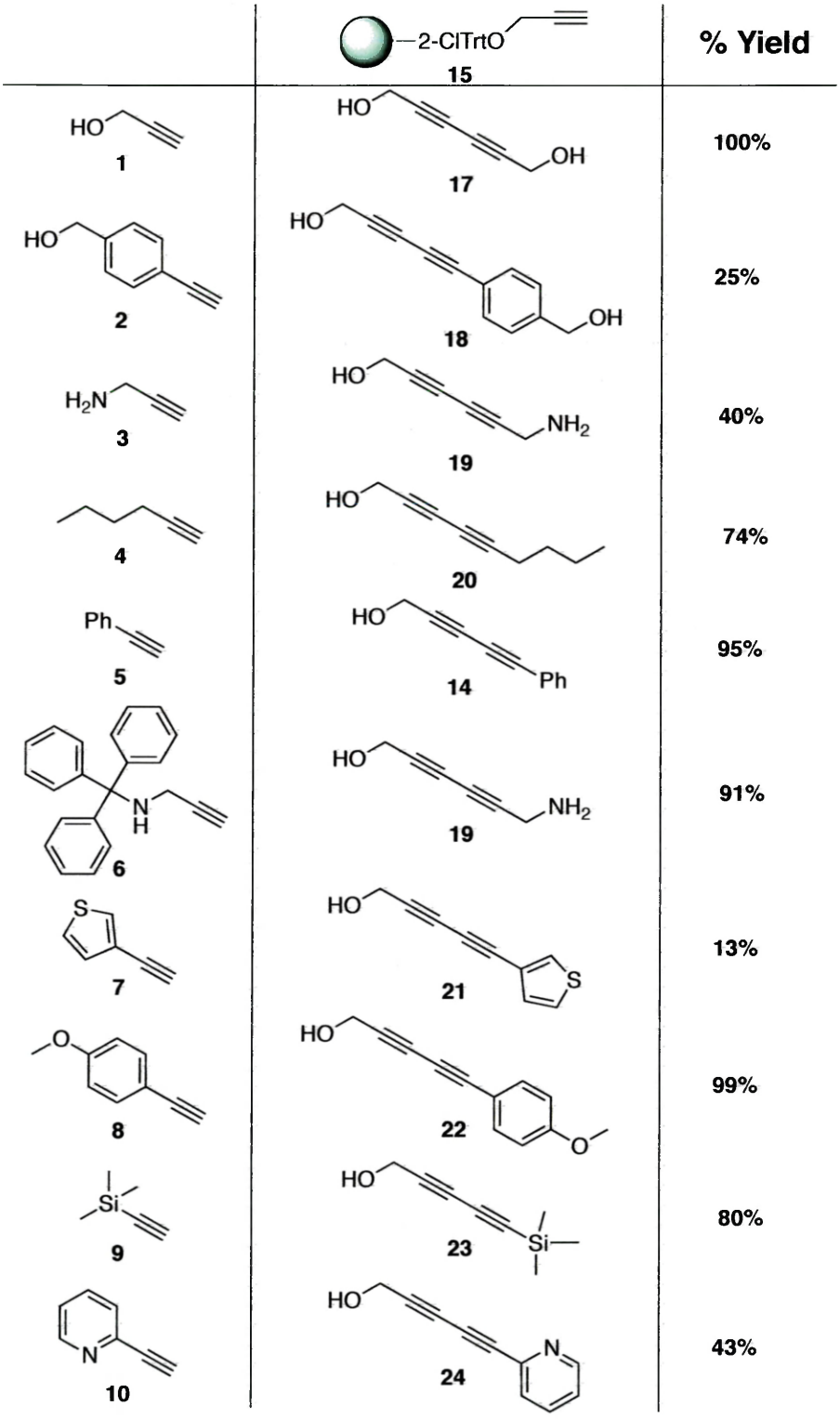

Table 2.1 – Library of diyne products generated through Glaser Hay coupling of immobilized propargyl alcohol with various alkynes.

The solid supported Glaser Hay coupling tolerated a variety of functionalities, including aromatic rings, silyl groups, free amines, alcohols, and alkyl chains. Alkynes containing free amine functionalities, such as **3**, were not as successful under the coupling conditions. However, a trityl-protected version, **6**, gave significantly higher yields of the desired -diyne product. Furthermore, the reaction with 2% TFA to cleave the product from the resin also removed the trityl protecting group on the amine, thereby yielding the same product as reaction with the free amine (Scheme 2.15).

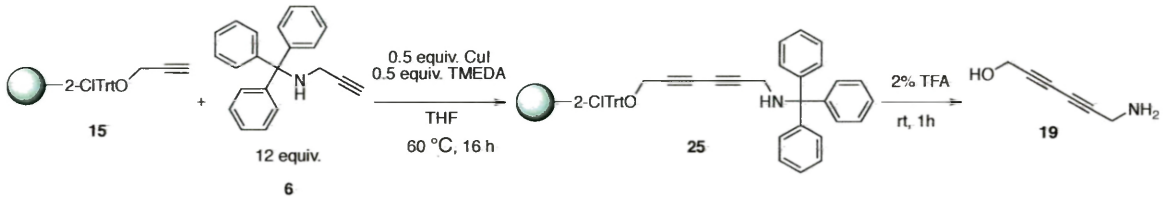

Scheme 2.15 – Solid support-assisted coupling of immobilized propargyl alcohol with an alkyne containing a protected amine moiety.

We hypothesize that the free amine functionality may have coordinated with the copper catalyst, reducing its activity within the reaction. By protecting this group with the trityl functionality, the coordination ability was minimized, resulting in a higher yield of the product **20**. Other interesting trends arose when analyzing the yields associated with the various products, most likely due to reactivity effects. While the anisole based **8** reacted well under the idealized conditions, the similar benzyl alcohol, **2**, had relatively lower yields. We speculated that the methoxy group of the anisole may serve as a protecting group for the alcohol, shielding it from other reactions with the copper catalyst. In contrast, the free alcohol of the benzyl alcohol was readily available, increasing the reactivity of the molecule, especially to form homodimers in solution. The 3-

ethynylthiophene reactant, **7**, was not well tolerated by the reaction conditions, likely due interaction of the nucleophile with the copper source.

Utilizing a propargyl amine derivatized resin, **26**, with the optimized coupling conditions we expanded the diyne library (Table 2.2). Less homodimer formation was observed with this resin, even at higher concentrations of loading, 0.9 mmol/g, indicating a lower reactivity than that observed with propargyl alcohol loaded resin.

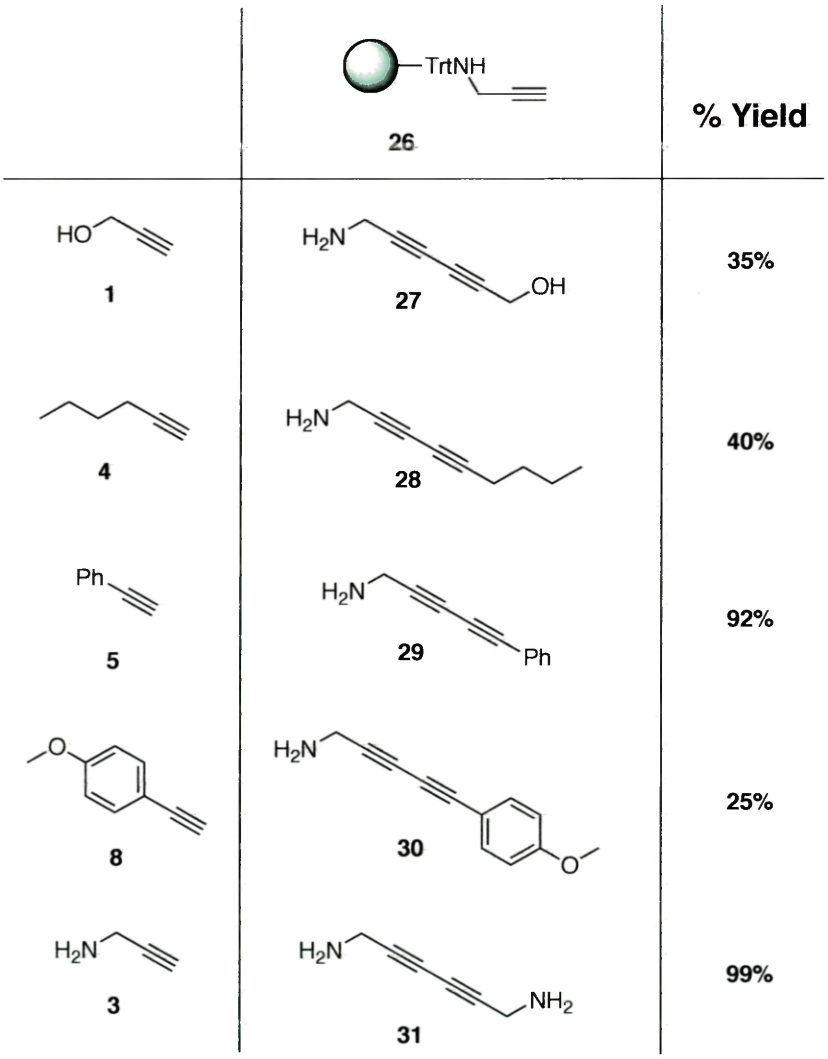

Table 2.2 – Immobilized propargyl amine coupled with multiple alkyne functionalities.

2.2.4 Future Directions for Solid Supported Couplings

Future work on this project aims to further expand the chemical library of available diynes. Unfortunately, we were unable to fully optimize the loading of 4-ethynylbenzyl alcohol (**2**) onto the 2-chlorotrityl resin, with large amounts of dimerization observed. After the formation of homodimer has been sufficiently suppressed for this immobilized alkyne, a variety of new compounds could be generated and analyzed. Overall, the formation of homodimer remains the main hindrance for this synthetic process, suggesting that the loading of the resin needs to be further optimized. By completely eliminating homodimer formation, this methodology would provide a rapid and efficient method for generating asymmetric diyne structures without requiring further purification steps.

2.2.5 Microwave-Mediated Glaser Hay Couplings

After generating a protocol for the solid-phase Glaser Hay couplings, we attempted to transition these reactions into a microwave reactor. We proposed that utilizing microwave technology, reaction times could be dramatically reduced from days to minutes. To this end, we attempted the standard coupling of the propargyl alcohol loaded resin, **15**, with phenylacetylene **8**, in a THF solvent system (Scheme 2.16). The THF also served as an ideal solvent for the microwave, due to its microwave transparency. In this way, reactions could be pulsed with varying intensities of microwave irradiation, without drastic increases in either pressure or temperature associated with solvent heating.

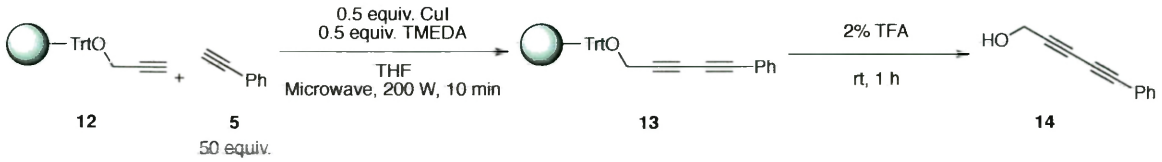

Scheme 2.16 – Solid support-assisted coupling under microwave conditions.

After investigating a variety of microwave power settings (100, 200, or 300 W), 200 W of power was selected since it produced the highest yields with minimal destruction of the resin. Unfortunately, when the optimized conditions were repeated in the microwave at 200 W for 10 min, there was a significant reduction in the yield of product to about 35%. This disparity between the yields for the thermal reactions compared to the microwave reactions suggests that the microwave setup may be negatively interacting with the resin. When dissolved in THF then pulsed with 200 W for 10 min, the reaction reached temperatures around 150 °C, possibly decomposing the resin and the catalyst.

This microwave-assisted methodology still requires slight modifications to the protocol before it can be gain widespread use. Once in the microwave reactor, the reaction must be stirred on a low setting in order to avoid physically damaging the resin. Additional work must also be conducted to combat the rising temperatures of the reaction that overheats the resin to the point of degradation. By improving the yields of these reactions while simultaneously decreasing the reaction times, the diverse diyne library could be generated in a rapid and efficient method perhaps rivaling the thermal counterpart.

2.3 Materials and Methods

General. Solvents and reagents were obtained from either Sigma-Aldrich or Fisher Scientific and used without further purification, unless noted. Tritylchloride resin, 100-200 mesh, 1% DVB crosslinking, was purchased from Advanced Chemtech. The 2-chlorotrityl chloride resin, 200-400 mesh, 2% DVB crosslinking, and the 2-chlorotrityl chloride resin, 200-400 mesh, 1% DVB crosslinking were purchased from Sigma-Aldrich. Terminal alkyne **6** was prepared according to literature procedures.[29] Reactions were conducted under ambient atmosphere with un-distilled solvents. NMR data was acquired on a Varian Gemini 400 MHz.

Immobilization of Propargyl Alcohol onto Trityl Chloride Resin in Low Loading Conditions

To flame dried vial was added trityl chloride resin (200 mg, 0.36 mmol, 1 equiv.) and dichloromethane (5 mL). The resin was swelled at room temperature with gentle stirring for 15 min. Propargyl alcohol (25.0 μL, 0.433 mmol, 1.2 equiv.) was added to reaction, followed by triethylamine (10.0 μL, 0.072 mmol, 0.2 equiv). The mixture was stirred at room temperature for 16 h. The resin was transferred to a syringe filter and washed with DCM and MeOH (5 alternating rinses with 5 mL each). The resin was swelled in CH_2Cl_2 and dried under vacuum for 45 min before further use.

Sample of Glaser Hay Coupling Protocol at 60 °C

Phenylacetylene (50.0 μL, 0.450 mmol, 50 equiv.) was added to a flame dried vial containing the propargyl alcohol derivatized trityl resin (50 mg, 0.035 mmol, 1 equiv.),

and tetrahydrofuran (0.750 mL). The copper catalyst (10 mg, 0.53 mmol, 0.59 equiv.) and tetramethylethylenediamine (10 μL, 0.066 mmol, 0.73 equiv.) were added to a separate flame-dried vial then dissolved in tetrahydrofuran (0.750 mL). The catalyst mixture was then added to the resin in one portion and stirred at 60 °C for 16 h. The resin was transferred to a syringe filter and washed with DCM and MeOH (5 alternating rinses with 5 mL each). The product was then cleaved from the resin by treatment with 1% TFA (DCM, 1 h), filtered into a vial. The solvent was removed *in vacuo* to give Compound **17** as a white solid (5 mg, 0.032 mmol, 95%).

Sample of Microwave-Assisted Glaser Hay Coupling on Propargyl Alcohol Resin

Propargyl alcohol-derivatized resin (50 mgs, 0.36 mmol, 1 equiv.) and phenylacetylene (100 μL, 1.8 mmol, 50 equiv.) were added to a microwave vial equipped with a stirring bar. The resin was swelled in solvent (1 mL) at room temperature for 15 min. CuI (10 mgs, 0.530 mmol, 0.59 equiv.), and tetramethylethylene diamine (10 μL, 0.66 mmol, 0.73 equiv.) were added to a flame-dried vial, dissolved in solvent (1 mL), and stirred until the metal was solubilized. The catalyst was added to the resin reaction in one portion then the vessel was sealed with a microwave cap. The reaction was irradiated in the microwave at a fixed power with slow stirring.

Analytical Data

5-phenylpenta-2,4-diyn-1-ol (14): The solvent was removed *in vacuo* to give compound **14** as a solid (4 mg, 0.036 mmol, 100%). ^{1}H NMR (400 MHz; $CDCl_3$): ∂ 7.49 (t, J = 5.9, 2H), 7.34-7.26 (m, 3H), 4.45 (s, 2H), 1.94 (s, 1H).

Hexa-2,4-diyne-1,6-diol (17): The solvent was removed *in vacuo* to give compound **17** as a white solid (5 mg, 0.032 mmol, 95%). ^{1}H NMR (400 MHz; $CDCl_3$): ∂ 4.36 (s, 4H).

5-(4-(Hydroxymethyl)phenyl)penta-2,4-diyn-1-ol (18): The solvent was removed *in vacuo* to give compound **18** as a solid (2 mg, 0.011 mmol, 25%). ^{1}H NMR (400 MHz; $CDCl_3$): ∂ 7.49 (dd, J = 8.0 Hz, 15.0 Hz, 4H). 4.72 (s, 2H), 4.35 (s, 2H).

6-Aminohexa-2,4-diyn-1-ol (19): The solvent was removed *in vacuo* to give compound **19** as a solid (3 mg, 0.014 mmol, 40%). ^{1}H NMR (400 MHz; CD_3OD): ∂ 5.21 (s, 2H), 4.35 (s, 2H), 3.39 (s, 2H).

Nona-2,4-diyn-1-ol (20): The solvent was removed *in vacuo* to give compound **20** as a solid (3 mg, 0.026 mmol, 74%). ^{1}H NMR (400 MHz; $CDCl_3$): ∂ 4.32 (s, 2H), 2.29 (t, J = 6.8 Hz, 3H), 1.52 (m, 2H), 1.42 (sextet, J = 7.2 Hz, 2H), 0.91 (t, J = 7.23 Hz, 3H).

5-(Thiophen-3-yl)penta-2,4-diyn-1-ol (21): The solvent was removed *in vacuo* to give compound **21** as a solid (1 mg, 0.006 mmol, 13%). ^{1}H NMR (400 MHz; $CDCl_3$): ∂ 7.58 (d, J = 2.3 Hz, 1H), 7.28 (s, 1H), 7.15 (d, J = 4.7 Hz, 1H), 4.42 (s, 2H).

5-(4-Methoxyphenyl)penta-2,4-diyn-1-ol (22): The solvent was removed *in vacuo* to give compound **22** as a solid (6 mg, 0.035 mmol, 99%). ^{1}H NMR (400 MHz; $CDCl_3$): ∂ 7.44 (d, J = 7.6 Hz, 2H), 6.85 (d, J = 7.62, 2H), 4.14 (s, 2H), 3.82 (s, 3H).

5-(Trimethylsilyl)penta-2,4-diyn-1-ol (23): The solvent was removed *in vacuo* to give compound **23** as a solid (4 mg, 0.026 mmol, 80%). ^{1}H NMR (400 MHz; $CDCl_3$): ∂ 4.33 (s, 2H), 0.20 (s, 9H).

5-(pyridin-2-yl)penta-2,4-diyn-1-ol (24): The solvent was removed *in vacuo* to give compound **24** as a solid (2 mg, 0.015 mmol, 43%). ^{1}H NMR (400 MHz; $CDCl_3$): ∂ 8.01 (d, J = 7.5 Hz, 1H), 7.65 (t, J = 7.4 Hz, 1H), 7.32 (t, J = 7.5 Hz, 1H), 6.91 (d, J = 7.4 Hz, 1H), 4.38 (s, 2H).

6-aminohexa-2,4-diyn-1-ol (27): The solvent was removed *in vacuo* to give compound **27** as a solid (6 mg, 0.025 mmol, 35%). ^{1}H NMR (400 MHz; CD_3OD): ∂ 5.21 (s, 2H), 4.35 (s, 2H), 3.39 (s, 2H).

Nona-2,4-diyn-1-amine (28):): The solvent was removed *in vacuo* to give compound **28** as a solid (7 mg, 0.029 mmol, 40%). ^{1}H NMR (400 MHz; CD_3OD): ∂ 5.24 (s, 2H), 3.41 (s, 2H), 2.29 (t, J = 6.8 Hz, 3H), 1.52 (m, 2H), 1.42 (sextet, J = 7.2 Hz, 2H), 0.91 (t, J = 7.23 Hz, 3H).

5-Phenylpenta-2,4-diyn-1-amine (29): The solvent was removed *in vacuo* to give compound **29** as a solid (17 mg, 0.066 mmol, 92%). ^{1}H NMR (400 MHz; CD_3OD): ∂ 7.49 (t, J = 5.9, 2H), 7.34-7.26 (m, 3H), 5.21 (s, 2H), 3.35 (s, 2H).

5-(4-Methoxyphenyl)penta-2,4-diyn-1-amine (30): The solvent was removed *in vacuo* to give compound **30** as a solid (5 mg, 0.018 mmol, 25%). ^{1}H NMR (400 MHz; CD_3OD): ∂ 7.34 (d, J = 7.62, 2H), 6.75 (d, J = 7.62, 2H), 5.14 (s, 2H), 3.82 (s, 3H), 3.39 (s, 2H).

Hexa-2,4-diyne-1,6-diamine (31): The solvent was removed *in vacuo* to give compound **31** as a solid (24 mg, 0.072 mmol, 99%). ^{1}H NMR (400 MHz; CD_3OD): ∂ 5.12 (s, 4H), 3.39 (s, 4H).

Chapter 3: Novel Mechanisms for Bacterial Transformations

3.1 Introduction

3.1.1 Bacterial Transformations

Introducing exogenous DNA into bacterial hosts is an extremely important technique in molecular biology. The hydrophilic, charged nature of DNA prevents it from readily crossing the bacterial cellular membrane. In order to facilitate the introduction of foreign DNA in the laboratory, cells must be induced into taking up the DNA, typically by making the membrane more permeable. Once the plasmid DNA is taken up by the cells, measures must be taken in order to ensure that the bacteria maintain the plasmid rather than releasing it. This is typically achieved by incorporating an antibiotic resistance gene into the plasmid, then forcing the bacteria to grow in the presence of the corresponding antibiotic. In order to survive in the environment, the cells must therefore maintain and express proteins encoded by the plasmid. Such transformations are essential in a variety of applications, including protein expression, molecular cloning, and mutagenesis. Though electroporation and chemical transformation are among the main methods for transforming bacteria, there are advantages and disadvantages inherent in each approach.

Electroporation consists of applying an electric field or pulse to a solution of cells in order to facilitate the uptake of substances, such as plasmid DNA. The brief shock alters the cellular membrane of the bacteria, disrupting the barrier long enough to allow plasmid DNA to enter the cell. The cell's natural mechanisms then repair the membrane before the cell dies from the stress. This specific method provides extremely efficient transformations typically on the order of ~10^8 colony forming units (cfu), however, it

requires the use of a specifically designed electroporation apparatus. Furthermore, electroporation relies on high-efficiency competent cells that must either be commercially attained or prepared in the laboratory. The preparation of such cells involves a tedious series of washes and manipulations in order to remove salts and other impurities that would affect the delivery of the electric pulse. Once prepared, the competent cells must be kept frozen at -80 ˚C and used within a certain amount of time. Chemical transformation offers a more economical option in which cells treated with calcium chloride are subjected to a short heat pulse at 42 ˚C in order to introduce exogenous DNA. The addition of the calcium chloride aids in the uptake of plasmid DNA, since the positively charged calcium ions coordinate the negatively charged backbone of DNA. The calcium is also proposed to simultaneously interact with the negative lipopolysaccharides on the surface of the bacterial cell. Though the complete mechanism of DNA uptake remains unclear, it is proposed that the presence of the salt ions coupled with the shock from the heat pulse generate pores within the cellular membrane. The plasmid DNA is able to pass through these pores, entering the cell before repairs can be made to the cellular membrane (Figure 3.1).[30]

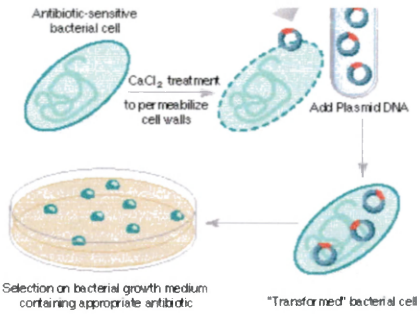

Figure 3.1 – Chemotransformation of bacterial cell in order to introduce exogenous DNA.[30]

Improvements to this technique have resulted in more efficient competent cells that give transformation efficiencies on the order of 10^6-10^7 cfu. Unfortunately, these cells also require substantial preparation in order to achieve desired levels of competency. Therefore, any improvements to enhance the utility and efficiencies of transformations should be welcome. To this end, we explored the use of microwave irradiation as a means to introduce exogenous DNA into *E. coli* without any tedious preparation of competent cells.

3.1.2 Microwave Irradiation in Biological Settings

While microwave irradiation has previously been exploited to enhance the rate, yield, and purity of synthetic reactions, it has more recently gained use in biological settings. The applications of these microwave-assisted methodologies include DNA hybridizations, polymerase chain reactions, and the activation of catalytic enzymes.[31,32,33] Given the significant dipoles present in biomacromolecules, especially with DNA and proteins, these species should respond to microwave irradiation. The dipole moments or ions within the solution would rotate to align with the oscillating electric field of the microwave and result in efficient heating of the system.

Bacterial transformation offers an ideal setting for the investigation of microwave technologies due to the pervasiveness of dipole moments, specifically in the form of nucleic acids, carbohydrates, phospholipids, and membrane-associated proteins. Previous reports explored the use of traditional microwave heating as a means of heat shocking cells during chemotransformations.[34] When prepared calcium chloride competent cells were irradiated at 180 W for 1 min in a conventional microwave oven, the transformation

efficiency, ~10^7 cfu, displayed a three-fold increase over traditional heat shocking at 42 °C. However, this microwave-improved transformation still required the tedious preparation of competent cells in order to yield successful transformants. Furthermore, conventional microwaves do not generate the focused microwave irradiation observed with specifically designed microwave reactors.

Based on these observations, we utilized a microwave reactor for transformations to better harness and direct the microwave energy while yielding more reproducible results. Under these conditions, the microwaves directly interact with the plasmid DNA and the dipoles within the cells, potentially improving the effectiveness of the transformations without the need for special preparation of cells.

3.2 Microwave-Assisted and Low Temperature Transformations

3.2.1 Development of Microwave-Mediated Bacterial Transformations

Given the role of bacterial transformation as a crucial tool in molecular biology, we aimed to develop new mechanisms for introducing exogenous DNA into cells. Our attempts focused on addressing issues associated with electroporation and chemotransformation protocols. The large dipole moments observed with biological settings prompted us to consider utilizing microwave technologies as a tool for improving the transformation process. In order to develop a microwave-assisted transformation protocol, an *E. coli* BL21 (DE3) strain of cells was grown to either log phase (OD_{600} 0.5) or stationary phase (OD_{600} 3.2). These two stages were selected to determine the best stage at which to harvest cells for the transformation process. We suspected that cells isolated during the log phase of growth would be more susceptible to the introduction of

DNA, since most competent cells for traditional transformations are harvested at an OD_{600} between 0.4-0.7. The stationary phase sample was chosen because we hypothesized that it would better withstand the cellular damage associated with the microwave-assisted protocol.

Once the cells reached the desired density they were then pelleted by centrifugation and resuspended in either 1:1 2xYT media/water or 1:1 2xYT media/glycerol. We proposed that the addition of glycerol to one set of cells might make them more resilient to the effects of the microwave irradiation due to its cryoprotectant nature. After this minimal preparation the cells were employed in the transformation process. An aliquot of cells was incubated on ice for 10 min with a pET-GFPWT plasmid containing an ampicillin resistance gene. After incubation, the cells were subjected to a brief pulse of microwave irradiation in a CEM Discover microwave reactor. Various pulse lengths (2s or 5s) and microwave intensities (50, 100, 150, 200, or 300 W) were assessed in order to determine ideal conditions for the transformations. The selected irradiation times in the microwave reactor were dramatically shorter than the 1 min pulses at 180 W reported in previous examples, since the microwave reactor generated more intensely focused beams than the previously used conventional kitchen microwaves. After each trial, the temperature achieved based on the pulse of microwave irradiation was recorded then appropriate controls were carried out in the absence of microwave irradiation. All of the transformation samples were recovered in 2xYT media for 1 h at 37 °C then plated on Luria-Bertani (LB) agar plated containing ampicillin.

Unfortunately, neither the microwave-pulsed samples nor the controls yielded viable bacterial colonies, indicating that the transformations were unsuccessful. In order

to confirm that the microwave irradiation did not decrease the viability of the cells, the same trials were conducted on cells without the addition of plasmid DNA. After recovery, the cells were plated on LB agar in the absence of any antibiotic and monitored for growth. No observable difference in growth was found between the microwave-pulsed cells and the non-irradiated controls, demonstrating that the brief microwave pulses were not decreasing cell viability and were not sufficient enough to transform non-competent cells.

Both the media/water samples and the media/glycerol samples were found to rapidly heat when subjected to the microwaves, even during the relatively brief pulses, often reaching above 60 °C. It was hypothesized that the heating arose from the presence of the aqueous media as well as the various ions in solution and their interactions with the applied electromagnetic field. Since these species were required for the transformation reactions, the experiments were transitioned to a CEM CoolMate system. The design of this instrument includes a jacketed reaction vessel that allows for the continuous flow of microwave-transparent solvent. The solvent can be pre-chilled to -50 °C such that the setup permits the use of microwave irradiation while simultaneously cooling the reaction (Figure 3.2).[35]

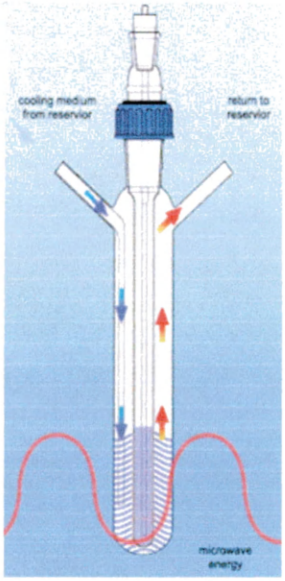

Figure 3.2 – The jacketed reaction vessel can be cooled with microwave transparent fluid, while the sample is irradiated with microwaves.[35]

After the microwave pulse, the CoolMate affords rapid cooling of the reaction, similar to the recovery of cells on ice after the heat-shock protocol in chemotransformations. Furthermore, the CoolMate provides a means for controlling the sample temperatures, thereby deconvoluting the temperature effects from the effects of the microwaves.

Again cells were grown to either log phase (OD_{600} 0.5) or early stationary phase (OD_{600} 1.0), then centrifuged and resuspended in either 1:1 2xYT media/water or 1:1 2xYT media/glycerol. The same pET-GFPWT plasmid containing ampicillin resistance was added (1μL) to the cells then the mixture was transferred directly to the CoolMate. Within the reactor, the reaction was cooled to (-30 ˚C or 0 ˚C) for about 1 min before being briefly pulsed (10-30 s) with microwaves (100, 200, or 300 W). After irradiation, the cells were recovered in 2xYT media for 1 h at 37 ˚C. Following the recovery, the cultures were plated in LB plates containing ampicillin and grown overnight. With these conditions, colonies were observed, indicating successful transformations. The number of

colonies for each set of conditions were counted and employed to determine the transformation efficiency (Figure 3.3) reported as cfu, colony forming unit.

$$TransformationEfficiency = ((\#\ ofcolonies)/ngDNAplated) * (1000ng/\mu L)$$

Figure 3.3 – Equation used to calculate the efficiency of a transformation.

The results from the CoolMate conditions listed in Table 3.1 indicate the relatively low efficiency of this method compared with previously reported transformation efficiencies. The samples grown to log phase (OD_{600} 0.5) yielded significantly higher efficiencies than those grown to stationary phase (OD_{600} 1.0), and are the only data listed in the table. Transformations conducted with the samples grown to stationary phase were unsuccessful, not producing viable colonies. Furthermore, the cells that were resuspended in 1:1 media/glycerol failed to produce bacterial colonies, giving an unsuccessful transformation. Only one such trial is listed in the table in order to provide a direct comparison to its 1:1 2xYT media/water counterpart that provided a transformation efficiency of 101 cfu. One major trend observed was that an increase in the power of the microwave pulse significantly increased the efficiency of the transformation. This phenomenon supported the idea that the microwave irradiation was the driving force behind the transformation, since the temperature of the microwave reactions remained the same regardless of the intensity used (100, 200, or 300 W).

Power	Time	Initial Temperature (°C)	Transformation Efficiency
0	10	0	0
0	30	0	0
0	10	-30	0
100	10	-30	24
200	10	-30	94
300	10	-30	94
300	15	-30	213
300	30	-30	101
300[a]	30	-30	0
300	60	-30	24
300[b]	2	25	0

Table 3.1 – Summary of transformation efficiencies for various CoolMate conditions. The samples were all grown to log phase (OD_{600} 0.5) prior to centrifugation and resuspension in 1:1 2xYT media/water, unless otherwise noted. All deviations were ± 9 cfu.

[a] Corresponds to the sample suspended in 1:1 media/glycerol

[b] Corresponds to the data from the CEM Discover trial, without cooling

The final row of Table 3.1 provides a sample of the conditions used with the CEM Discover microwave reactor, which lacks a cooling component, and subsequently reached 50 °C during the pulse sequence. This direct comparison with the transformations conducted in the CEM CoolMate reveals the importance of the cooling during the transformation process. However, the -30 °C was not sufficient to elicit a transformation as seen by the control that was subjected to no microwave irradiation for 10 s in the microwave reactor. These conditions did not afford bacterial colonies after the transformation, indicating that the microwave irradiation plays a crucial role in the cellular uptake of plasmid DNA. Another set of conditions included using a -30 °C bath followed by a transfer to a conventional heating block in order to better reflect the microwave temperature profile (Figure 3.4). Again, these transformation attempts yielded

no bacterial colony growth, thereby confirming the role of the microwave irradiation over cryogenic effects in the transformation process.

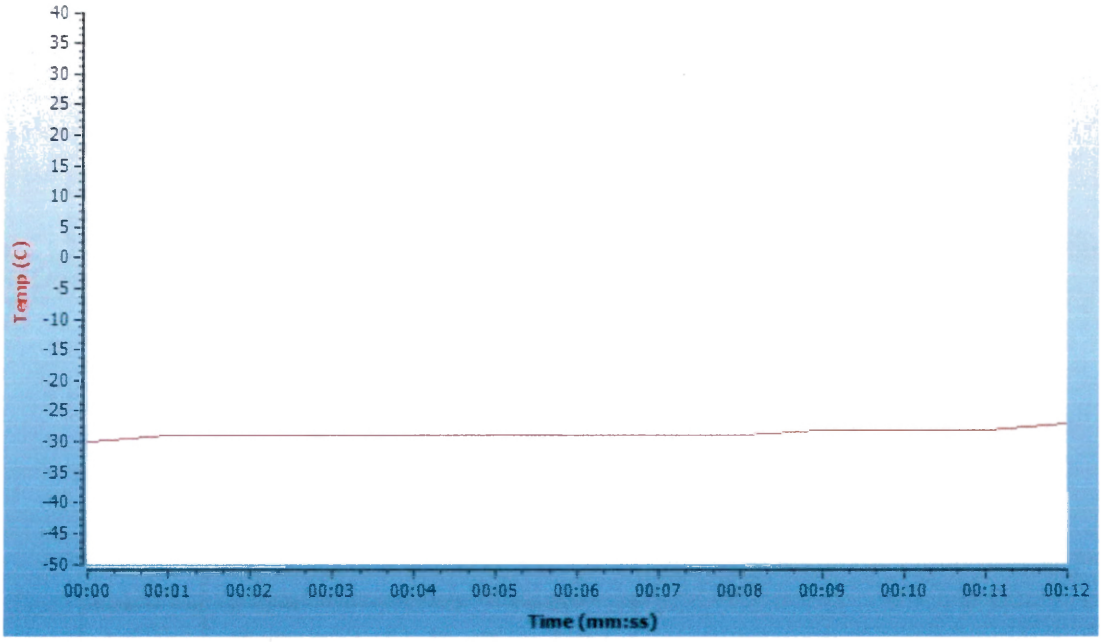

Figure 3.4 – A sample of the temperature profile reported during a 10 s CoolMate transformation.

Overall, the highest transformation efficiency, 213 cfu, was recorded for cells that were cooled to -30 °C, then pulsed at 300 W for 15 s. While the efficiencies remained relatively low when compared with existing methods, the results emphasize the potential for the use of microwaves to promote DNA transformations. We hypothesized that the microwave irradiation at higher powers caused sufficient perturbation to the bacterial membranes to elicit the effective uptake of foreign DNA, without compromising the cell viability.

To ensure that the growth of colonies was indeed due to the uptake of the desired plasmid, a transformed colony was selected and grown to stationary log phase (OD_{600} 3.2).

The cells were then harvested and the plasmid was re-isolated using a DNA purification kit. The resulting plasmid was digested with a restriction enzyme, EcoRI-HF, in order to yield linear DNA for gel electrophoresis. To visualize the presence of the desired plasmid, the DNA sample was loaded and run on a 1% agarose gel. The gel was then imaged on a UV-Vis transilluminator. The plasmid was observed as a dark band at about ~4.5 kb, the expected size for the pETGFP-WT (Figure 3.5).[36]

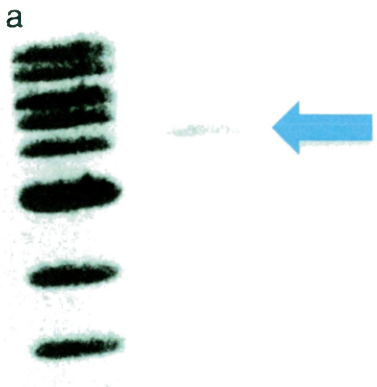

Figure 3.5 – Confirmation of successful transformation plasmid uptake, with the sample corresponding to 4.5 kb (right band) compared to the standard ladder (left).

Additionally, cells exposed to microwave irradiation during the transformation process were assessed for their ability to express viable protein. Expression of viable protein ensures that the plasmid DNA and the bacterial cells were undamaged or mutated by the microwave irradiation. After selecting a colony, cultures were grown and utilized to express the green fluorescent protein, and the corresponding protein was isolated. The protein was then confirmed to be a functional, fluorescent protein by analysis on an SDS PAGE gel (Figure 3.6).

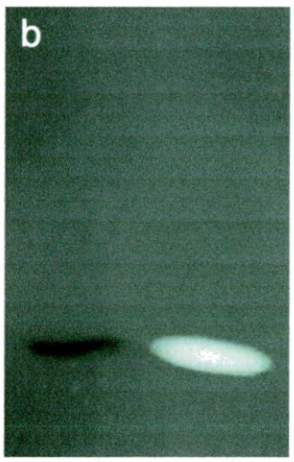

Figure 3.6 – Analysis of protein expression by SDS PAGE. The fluorescent band (right) corresponds to the desired green fluorescent protein (GFP), while the darker band (left) gives the protein ladder standard.

To this end, we successfully utilized microwave irradiation to transfer plasmid DNA into E. coli cells, while maintaining cellular function and protein expression. Furthermore, the results of this study highlight the potential for further investigations coupling microwave irradiation with biological settings.

3.2.2 Optimization of Liquid Nitrogen Transformations

To better mimic the temperature profile within the CoolMate, multiple controls were investigated in the absence of microwave irradiation. To investigate the optimal transformation protocol, cells were rapidly frozen with plasmid by submerging the cells in liquid nitrogen (-196 °C), cooling them far below the -30 °C of the CoolMate. After a standard recovery phase, the cells were plated on ampicillin containing LB agar plates and afforded a relatively high transformation efficiency of ~10^4 cfu. Even though low-temperature transformations were originally observed in 1972, very few protocols have been developed for this technique, especially in comparison to methods for both

electroporation and heat shocking.[37] These low-temperature transformations have found their primary use in *Agrobacterium tumefaciens*, but have not effectively been adapted for widespread use in *E. coli* systems.[38,39] While Takahashi *et al.* developed a freeze-thaw procedure for non-competent *E. coli* strains, the transformation efficiencies were relatively low ~10^2 cfu.[40] Additional investigation revealed that the same freeze-thaw procedure generated efficiencies approaching ~10^6 cfu, however this required additional preparation of competent cells.[41,42]

Our results indicated a mechanism to advance to the technique of low-temperature transformation by eliminating the tedious and often expensive preparation of competent cells, while still yielding relatively high transformation efficiencies. To better optimize the freeze-thaw transformations we adjusted multiple variables within the transformation process, including the freezing temperature, the density of the bacterial cells, and the number of freeze-thaw cycles.

Based on the results that were observed during the CoolMate transformations, an *E. coli* BL21 (DE3) strain of cells was selected and grown to log phase with an OD_{600} of 0.6. Cells grown to this density consistently yielded relatively higher transformation efficiencies, compared to cells isolated during the early and late stationary phases. By initially utilizing this cell density, we were better able to investigate the role of other factors. After obtaining the desired density, the cells were pelleted by centrifugation then resuspended in either 1:1 2xYT media/water or 1:1 2xYT media/glycerol as before. The cells were incubated on ice for 10 min with a pET-GFPWT plasmid then submerged in a coolant for 20 s. A variety of cooling baths were assembled in order to explore a range of freezing temperatures. A -30 °C environment was achieved by placing the cells

in the CoolMate vessel after it had been chilled to the appropriate temperature. Acetonitrile and dry ice were combined to afford a -42 °C bath, while dry ice and acetone where mixed to reach -72 °C. A mixture of methanol and liquid nitrogen served as a -94 °C bath and a pure liquid nitrogen bath was employed to achieve -196 °C.

Each sample was thawed on ice after the freezing period then recovered in 2xYT media for 1 h at 37 °C. The cultures were plated, grown, and assessed for the efficiency of the transformation conditions. Only the samples that were resuspended in 1:1 media/water produced viable colonies, while the samples containing 1:1 media/glycerol consistently yielded no transformants. The results and conditions for the successful transformations are summarized in Table 3.2.

Competent Cell OD_{600}	Freeze Temperature (°C)	Transformation Efficiency
0.6	-30	0
0.6	-42	38
0.6	-78	$1.6x10^2$
0.6	-94	$1.2x10^3$
0.6	-196	$2.2x10^5$

Table 3.2 – Transformation efficiencies for specific freezing temperatures. All deviations were ± $1.2x10^1$ cfu.

The -196 °C freezing bath generated the highest transformation efficiency of $2.2x10^5$ cfu, nearly as successful as other low-temperature transformation methods. An increase in the freeze temperature drastically decreased the transformation efficiency, with any temperature above -42 °C not yielding any colonies. As a result, further improvement of the liquid nitrogen-assisted transformations became our primary focus.

We then re-examined the role of cell density by growing the cultures to a variety of OD_{600} stages before centrifugation, resuspension, and transformation. To account for any variance in cell concentration, all of the samples were resuspended in a volume that would give a final OD_{600} of 27.7, then portioned into 100 μL aliquots. Each sample was incubated with pET-GFPWT then immersed in liquid nitrogen for 20 s. After the recovery process, only the samples in a 1:1 media/water mixture afforded bacterial growth and were reviewed for relative efficiencies (Table 3.3).

Competent Cell OD_{600}	Freeze Temperature (°C)	Transformation Efficiency
0.1	-196	$5.2x10^3$
0.2	-196	$2.8x10^5$
0.4	-196	$8.4x10^4$
0.6	-196	$2.2x10^5$
0.8	-196	$1.6x10^3$
1.0	-196	$5.0x10^3$
3.0	-196	$7.2x10^3$

Table 3.3 – Transformation efficiencies for various cell densities. All deviations were ± $1.4x10^1$ cfu.

Though all of the transformation conditions were more successful than those reported by Takahashi *et al.*, the highest efficiency corresponded to an OD_{600} of 0.2.[8] This value was similar to the densities required for both chemically competent and electro-competent cells; however, our method removes the tedious competent cell preparations that are necessary with the other techniques.

Given the high efficiencies observed with a single freeze-thaw cycle in liquid nitrogen, we proposed that additional freeze-thaw cycles might further enhance the transformation abilities of this method. To evaluate the reproducibility of any

improvements to the efficiencies and to ensure the optimization of the cell density, we grew cultures to various growth time points and resuspended to afford samples with a final OD_{600} of 27.7. For continuity, samples were resuspended in either 1:1 media/glycerol or 1:1 media/water. After addition of the pET-GFPWT plasmid, cells were either subjected to one or 2 freeze-thaw cycles prior to recovery. Though cells resuspended in 1:1 media/glycerol were unsuccessful, the transformation efficiencies for the 1:1 media/water samples are reported in Table 3.4.

Competent Cell OD_{600}	Freeze-Thaw Cycles	Freeze Temperature (°C)	Transformation Efficiency
0.1	1	-196	$5.2x10^3$
0.1	2	-196	$2.9x10^4$
0.2	1	-196	$2.8x10^5$
0.2	2	-196	$2.8x10^5$
0.4	1	-196	$8.4x10^4$
0.4	2	-196	$2.3x10^5$
0.6	1	-196	$2.2x10^5$
0.6	2	-196	$3.7x10^5$
0.8	1	-196	$1.6x10^3$
0.8	2	-196	$3.5x10^4$
1.0	1	-196	$5.0x10^3$
1.0	2	-196	$4.8x10^4$

Table 3.4 – Transformation efficiencies for various cell densities when subjected to either one or two freeze-thaw cycles in liquid nitrogen.

Ultimately, the cells grown to an OD_{600} of 0.6 and exposed to two cycles of liquid nitrogen freezing provided the optimal efficiency of $3.6x10^5$ cfu. For a majority of the samples, an additional freeze-thaw cycle improved the transformation efficiency, with some samples increasing a full order of magnitude. We theorized that this advancement may be due to the compounded effect that two cycles of freezing have for disrupting the

bacterial membrane. When the cells were subjected to three freeze-thaw cycles, the transformation efficiencies drastically decreased to ~10^1, with four or more freeze-thaw cycles failing to yield any viable colonies.

Combining all of the idealized conditions, we incorporated various divalent salts with the aim of further improving the effectiveness of the liquid nitrogen-assisted transformations. Even small concentrations of divalent salts have been documented to serve as useful buffers; shielding the negatively charged phospodiester backbone of DNA.[43] A solution containing 10 mM specific cation, NH_4Cl, $MgCl_2$ or $CaCl_2$, was added to the growth media prior to centrifugation and resuspension of the cells. Multiple freeze-thaw cycles as well as various freeze temperatures were also studied with these cells (Table 3.5).

Competent Cell OD_{600}	Freeze-Thaw Cycles	Cation Additive	Freeze Temperature (°C)	Transformation Efficiency
0.6	1	-	-196	$1.3x10^5$
0.6	2	-	-196	$2.4x10^5$
0.6	1	-	-42	$5.2x10^2$
0.6	1	NH_4Cl	-196	$4.7x10^4$
0.6	2	NH_4Cl	-196	$8.9x10^4$
0.6	1	NH_4Cl	-42	0
0.6	1	$MgCl_2$	-196	$3.4x10^4$
0.6	2	$MgCl_2$	-196	$1.5x10^5$
0.6	1	$MgCl_2$	-42	$5.2x10^2$
0.6	1	$CaCl_2$	-196	$9.6x10^4$
0.6	2	$CaCl_2$	-196	$1.1x10^5$
0.6	1	$CaCl_2$	-42	$1.1x10^3$

Table 3.5 – Comparison of transformation efficiencies in the presence or absence of divalent cations.

The inclusion of NH_4Cl in the growth media negatively impacted the transformation efficiency, however it did not completely hinder the transformation. Furthermore, the presence of Mg^{2+} or Ca^{2+} ions did not significantly enhance the transformations compared to the samples without supplemental cations.

Overall, the optimized transformation conditions involved the growth of cell cultures to an OD_{600} of 0.5-0.6 followed by concentration in a media/water mixture. For the freezing protocol, the ideal conditions require the cells to be subjected to two cycles of freezing in liquid nitrogen.

3.2.3 Exploring the Versatility of Liquid Nitrogen-Assisted Transformations

To explore the versatility of the optimized methodology, we probed the application of liquid nitrogen-assisted transformations with varying plasmid sizes, antibiotic resistances, and bacterial species. In addition to the original pET-GFPWT plasmid, a pET-22 plasmid and an SsoWT plasmid were utilized under the developed transformation conditions. While these plasmids harbor different origins of replications as well as antibiotic resistances, with sizes ranging from 4.5 kb to 5.5 kb, they were consistently transformed with liquid nitrogen to give high yields, $\sim 10^5$. Furthermore, this transformation technique was successfully employed to perform a simultaneous double transformation of two plasmids, with an uptake efficiency of $\sim 10^2$ cfu. This is expected due to the difficult nature of double transformations. Though double transformations typically have efficiencies on the order of $\sim 10^5$, the liquid nitrogen method still offers a practical means of introducing a wide array of plasmids into cells. For laboratory purposes, one bacterial transformant is sufficient to conduct further biological assays and

techniques, including protein expression and large-scale plasmid isolation. Moreover, the removal of advanced cell preparation prior to transformation as well as additional equipment, such as an electroporator, allows this method to have widespread applications in virtually any laboratory.

A broader application of the protocol involved the transformation of exogenous DNA into a separate species of bacteria, *Myobacterium smegmatis*. This host cell line offers a more significant challenge during transformations since the cells contain a more complicated cell wall as well as poor genetic transfer systems.[44] Currently, few methods exist for introducing exogenous DNA into these systems, posing an incredible challenge for research on the variety of diseases associated with these organisms. Competent cells were prepared for both organisms and transformed utilizing previously developed electroporation techniques in order to quantify efficiencies for these standard methods. Aliquots of our cell cultures with minimal preparation were also subjected to identical electroporation protocols, however the high salt content of the media resulted in arching of the sample and subsequent killing of the cells. After transformations of *M. smegmatis* with the CoolMate protocol failed to yield viable colonies, we proposed that the robust nature of the *M. smegmatis* cells likely increased their resistance to the damage caused by microwave irradiation. Utilizing the low-temperature method developed for the liquid nitrogen-mediated transformation of *E. coli*, a pMycVec 1 plasmid (5.9 kb) was successfully transformed into *M. smegmatis* cells (Table 3.6).[45]

Organism	Electroporation with competent cell	Electroporation with noncompetent cells	Freeze-thaw transformation	CoolMate Transformation
E. coli	$1.9x10^9$	-	$3.7x10^5$	$2.1x10^2$
M. smegmatis	$1.1x10^5$	-	$6.9x10^3$	-

Table 3.6 – Efficiencies for both host organisms utilizing existing transformation protocols, as well as our optimized transformation conditions.

The success of the freeze-thaw transformation method for both *E. coli* and *M. smegmatis* reveals an efficient method for introducing exogenous DNA without requiring any significant preparation of cells. The lower efficiencies reported in *M. smegmatis* compared to those in *E. coli* were anticipated due to the more complex nature of the *M. smegmatis* cell wall. This trend was further reflected in the efficiencies of electroporation transformation with competent cell stocks, with *M. smegmatis* displaying a ~10^4 decrease in efficiency compared to the identical transformation in *E. coli*. The development of this simple, yet effective transformation technique in both species represents a significant advance to the field.

3.2.4 Hypothesized Mechanism for Low-Temperature Transformations

Throughout the development of this methodology, the samples containing glycerol in place of water consistently failed to produce successful transformants; even under the most-optimized protocol. Given the cryoprotectant nature of glycerol, typically exploited in molecular biology, this tendency indicates that the successful low-temperature transformations may result from the rapid formation of ice crystals. Without the glycerol protectant, samples that were submerged in the liquid nitrogen bath

experienced rapid cooling, resulting in disruption of the bacterial cell wall. This mechanism is further substantiated by the trends observed in the temperature optimization.

3.2.5 Conclusions and Future Directions

Herein we report the development of two efficient methods for the introduction of foreign DNA into bacterial cells, specifically *E. coli*. Both techniques demonstrate potential for widespread use in molecular biology and chemistry, specifically due to the minimal cell preparation and the relatively high transformation efficiencies. Furthermore, the microwave-assisted transformation method hints at the potential applicability of microwave irradiation on complex biological systems. The simplified freeze-thaw procedure offered high reproduciblity and time saving results that were easily adapted to multiple bacterial species. Moreover, the versatility of the liquid nitrogen-assisted transformations has allowed for a significant improvement in the delivery of DNA into more resilient organisms, such as myobacteria.

Future work in this area aims to better understand the mechanisms for both low-temperature and microwave-assisted transformations. Armed with this knowledge, transformation conditions could be better optimized for a given organism or plasmid, especially with regards to the liquid-nitrogen method. The results for the microwave-mediated method, specifically the CoolMate transformations, indicate that biological molecules and environments hold vast potential for utilization with microwave technologies. The dipoles within these systems\ display significant interactions with microwave irradiation and should be explored for further applications.

3.3 Materials and Methods for Bacterial Transformations

General. Solvents and reagents were obtained from either Sigma-Aldrich or Fisher Scientific and used without further purification, unless noted. *Escherichia coli* BL21(DE3) cell lines were obtained from Novagen. The various plasmids utilized during the transformations were obtained through either collaborators or Novagen.

Optimized Preparation of Competent Cells

2xYT media (4 mL) was inoculated with *Escherichia coli* Novagen BL21(DE3) strain of cells and then incubated for 16 h at 37 °C to stationary phase. The starter culture (1 mL) was then added to fresh 2xYT media (100 mL) and incubated with vigorous shaking at 37 °C and monitored by routine optical density measurements on a spectrophotometer at 600 nm to assess bacterial growth. At the desired density, the culture was centrifuged at 4,000 rpm for 20 min. The resulting cell pellet was resuspended in either deionized water or glycerol, for a final cell optical density of 27.7. The resuspended cells were then aliquoted (100 μL each) and kept on ice.

Liquid Nitrogen Transformation

An aliquot of BL21(DE3) cells was kept on ice, and plasmid DNA (1 μL, 70 μg) was added. The cells were incubated on ice for 5 min and then submerged in liquid nitrogen for 20 s. After thawing, the cells were either subjected to a second freeze cycle or recovered in 2xYT media (500 μL), followed by 1 h of incubation at 37 °C. Cells were then plated on Luria-Betani agar (LB) plates containing appropriate antibiotics and

incubated overnight at 37 °C. Colonies were counted to assess transformation efficiency, and individual colonies from these plates were selected to ensure the presence of plasmid DNA.

Microwave CoolMate Transformation

An aliquot of BL21 (DE3) cells was kept on ice, and plasmid DNA (1 μL, 70 μg) was added. The cells were incubated on ice for 5 min and then placed in a Discover CoolMate vessel. Each sample was cooled in the CoolMate to a specific temperature (typically −30 °C) before it was subjected to microwave radiation and simultaneous cooling. The temperature was monitored using a fiber optic probe, and upon the conclusion of the microwave pulse, the sample was removed from the vessel and thawed to room temperature. The cells were recovered in 2xYT media (500 μL), followed by 1 h of incubation at 37 °C. Cells were then plated on LB plates containing appropriate antibiotics and incubated overnight at 37 °C. Colonies were counted to assess transformation efficiency, and individual colonies from these plates were selected to ensure the presence of plasmid DNA.

Re-Isolation of Plasmid

A single colony was picked from the GFP-LB-Amp plate and used to inoculate 2xYT media (4 mL) containing ampicillin. After growing overnight at 37 °C, the culture was centrifuged at 4000 rpm for 15 minutes. The cell pellet was then mini-prepped using a QIAGEN® Mini-prep Kit. The resulting plasmid was digested with either EcoRI-HF, BamHI-HF, or HindIII-HF (1 μL); NEBuffer 4 (5 μL); and BSA (1μL) (50 μL total

volume). The digestion reaction was incubated at 37 °C for 1 hour. The enzyme was then inactivated at 80 °C for 20 minutes. A 1% agarose gel was poured and 10 μL of a digest reaction was loaded (with 2 μL 6X loading dye) and run (120 V; 30 min) in 1X TAE. The gel was visualized and photographed on a UV-Vis transilluminator.

Assessment of Viable Protein Expression

A pET-101 Green Fluorescent Protein (GFP) plasmid was added to competent BL21(DE3) cells (100 μL; Novagen). The cells were transformed using either the previously described liquid nitrogen or microwave technique, then plated on LB agar containing ampicillin and grown overnight at 37 °C. A single colony was then used to inoculate 2xYT containing 50 μg/mL ampicillin (4 mL). After growing overnight at 37 °C, the starter culture (700 μL) was used to inoculate two 2xYT media containing ampicillin (10 mL ea.). These expression cultures were incubated with shaking at 37 °C until the OD_{600} reached 0.7. At this point, one of the expression cultures was induced with 1M IPTG (10 μL). The cultures were then grown for 16 hours at 30°C. Both expression cultures were pelleted at 4000 rpm for 20 minutes, and then frozen at -80 °C for 20 minutes. The cell pellets were resuspended in Bug Buster (500 μL; Novagen) supplemented with lysozyme to lyse the cells. The cell mixture was incubated at room temperature for 20 minutes, and then centrifuged at 13,000 rpm for 20 minutes. The supernatant was then added from the QIAGEN® Ni-NTA Spin Column, and GFP was purified according to the manufacturer's protocols. GFP expression was assessed by SDS-PAGE with an 8% resolving gel (150 V, 60 min).

Chapter 4: Unnatural Amino Acids

4.1 Introduction

4.1.1 Expanding the Genetic Code

All currently known organisms employ the same 20 natural amino acids encoded with the same genetic code. These canonical amino acids allow proteins to perform a wide variety of activities ranging from transcription to mounting an immune response. However, amino acids themselves are rather limited in terms of chemical functionality. As a result, many proteins must undergo posttranslational modifications such as phosphorylation or cofactor attachment in order to complete their necessary functions.[46]

Researchers have recently attempted to expand the genetic code in various organisms in an effort to uncover novel protein dynamics, as well as enhance known protein activities.[47] Incorporation of amino acids with diverse chemical moieties, allows for more thorough investigation of the correlation between protein structure and function. Furthermore, these unnatural amino acids often improve the overall function of the protein, through increased binding of substrates or enhanced catalytic activity.[48]

To date, there are hundreds of amino acid derivatives which possess a large variety of chemical modifications readily available for purchase. Unnatural amino acid side chains containing azides, fluorophores, or metals have been synthesized and successfully incorporated into various host organisms.[49,50]

4.1.2 Biological Translation of Proteins

Translation is a biological process in which messenger RNA (mRNA) serves as a

template for the production of a polypeptide chain or protein on the ribosome with the assistance of a translational RNA (tRNA). This process requires the combination of multiple components, converting a nucleotide template sequence to a polypeptide product. In naturally occurring translation, the genetic code assigns a specific amino acid to each triplet codon within an mRNA sequence. The amino acid must first be charged or physically attached to an aminoacyl-tRNA. The formation of a charged aminoacyl-tRNA requires an aminoacyl tRNA synthetase (aaRS) loading a specific amino acid onto an isoacceptor tRNA or empty tRNA.[51] A unique, orthogonal aaRS exists for each amino acid, responsible for charging that amino acid onto its cognate iso-tRNA (Figure 4.1).[52]

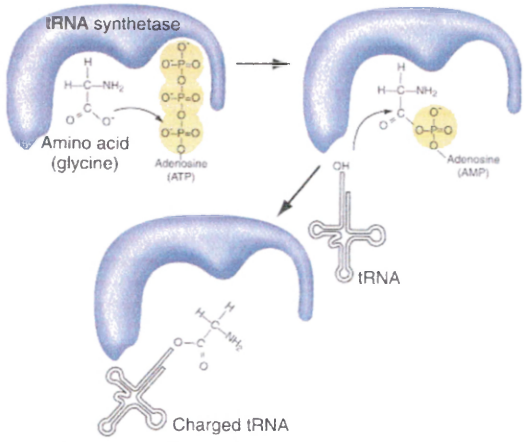

Figure 4.1 – A tRNA synthetase charging an amino acid onto an iso-tRNA in the presence of ATP.[52]

Once the tRNA contains the proper amino acid, it can interact with the ribosome to convert the nucleotide mRNA sequence into a peptide product. To accomplish this, the aminoacyl-tRNA complimentary base pairs a particular anti-codon loop with the mRNA triplet codon (Figure 4.2).[53]

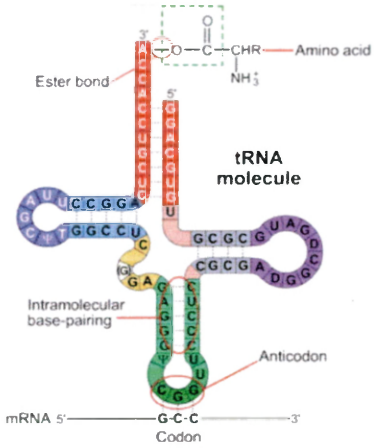

Figure 4.2 – Translation RNA (tRNA) molecule with anticodon loop base pairing with the three-base codon present in the mRNA sequence.[53]

Within the anti-codon loop, only the first two nucleotides Watson-Crick base pair with the mRNA codon. The third nucleotide within the sequence is less selective in its base pairing, sometimes referred to as "wobbling".[54] This phenomenon allows a single tRNA species to pair with more than one mRNA codon and overcome the degeneracy inherent in the genetic code.

4.1.3 Manipulating the Translational Machinery

While many methodologies have been proposed in order to incorporate unnatural amino acids *in vivo,* one of the most successful approaches manipulates the translational machinery to in order to site-specifically encode for the unnatural amino acid. For the addition of a new amino acid to be successful it must be loaded onto a tRNA that will insert it in response to a specific codon.[51] This specific tRNA must not be recognized by native *E. coli* aminoacyl-tRNA synthetases, so that none of the native amino acids will be loaded onto the tRNA. Conversely, a synthetase is required that does not recognize

naturally occurring tRNAs. One of the most efficient methods of generating an orthogonal aaRS/iso-tRNA pair in *E. coli* is to import a heterologous pair from a eukaryote or archaeon, such as *Methanococcus jannashii*.[46] This ensures that the native synthetase, or aaRS, will not load amino acids onto endogenous *E. coli* iso-tRNAs and, similarly, that the native aaRSs will not recognize the foreign iso-tRNA. Typically, the aaRSs for unnatural amino acids are evolved by site-mutation and selection. Ultimately, the active site of the aaRS must structurally recognize the three-dimensional conformation of the unnatural amino acid. To this end, several orthogonal pairs have been adapted and improved for use in *E. coli* hosts.[46]

Once this new translation machinery is incorporated there must be an mRNA codon for the loaded aaRS to base pair with, thereby inserting the unnatural amino acid at a specific site. The TAG triplet, or amber stop codon typically serves as a codon that terminates translation; however, it is rarely used in most organisms and can be exploited to site specifically incorporate a desired unnatural amino acid.[55] The anticodon sequence of the eukaryote or archaeon tRNA is mutated so that it recognizes the amber stop codon through complementary base pairing; allowing for site specific *in vivo* addition of the amino acid into the protein by the ribosome. This allows the translation machinery to "read through" the codon and produce full-length protein instead (Figure 4.3).[56]

After several rounds of engineering and selections, researchers are able to evolve an aaRS/tRNA pair that incorporates a specific unnatural amino acid in response to a TAG codon.[55] An added benefit is that if the unnatural amino acid is not substituted at this codon, then the protein will be prematurely terminated. After successful incorporation of the modified translation machinery, as well as the necessary unnatural amino acid, a

protein containing a site-specific unnatural amino acid can be synthesized *in vivo*.[53]

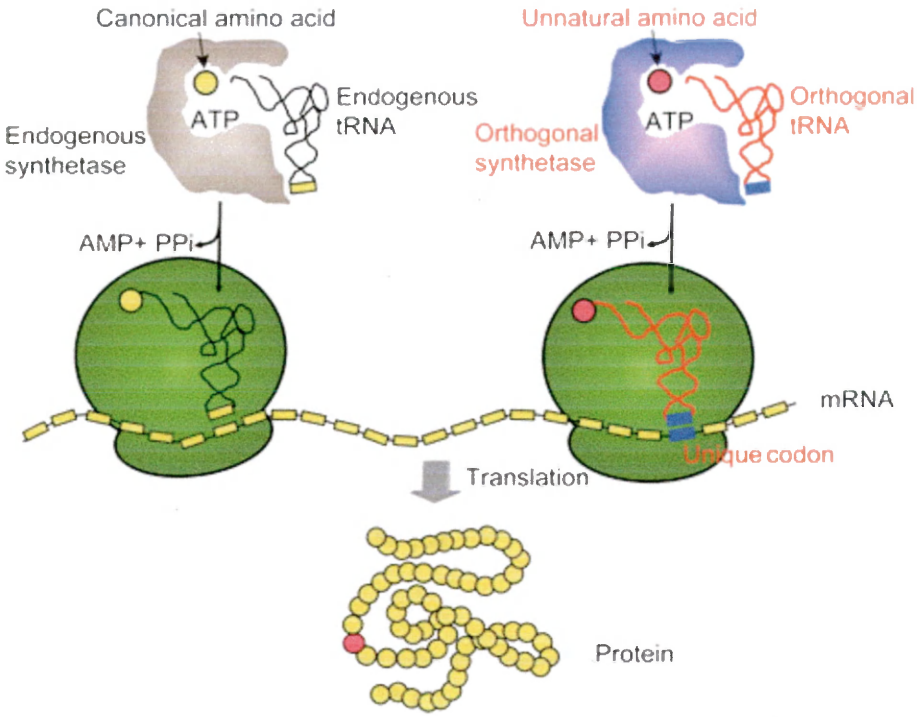

Figure 4.3 - In normal translation, the tRNA synthetase charges an amino acid (yellow) to a specific tRNA. This charged tRNA subsequently complementary base pairs with a codon within the mRNA, adding a natural amino acid to the growing peptide. For an unnatural amino acid (pink), the orthogonal tRNA synthetase charges the unnatural amino acid onto the orthogonal tRNA. This tRNA next interacts with a unique TAG codon within the mRNA, to site-specifically deliver the unnatural amino acid. Ultimately a protein is produced with the unnatural amino acid (pink) incorporated at a specific site.[53]

Experimentally, the utilization of this method with the modified translation machinery requires two separate plasmid; one plasmid that contains the gene for the aaRS pair, and one that encodes for a protein containing a TAG codon. When cells containing the necessary plasmids are grown and expressed in media containing the unnatural amino acid, relatively large amounts of unnatural protein can be produced *in vivo*.

4.1.4 Fluorotyrosine Based Unnatural Amino Acids

Wide arrays of unnatural amino acids have been successfully incorporated into green fluorescent protein (GFP) at various positions within the protein.[57] The overall structure of GFP consists of a beta barrel structure containing a covalently bonded chromophore within the center (Figure 4.4).[58] Many unnatural amino acids have previously been expressed on the surface of the protein, as part of the beta barrel, in order to provide functional chemical handles or novel applications.

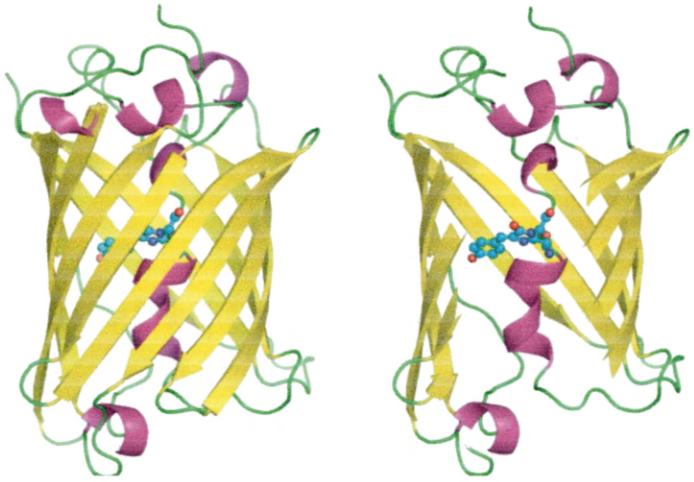

Figure 4.4 – Three-dimensional structure of green fluorescent protein (GFP) with the beta barrel (yellow) and the chromophore core (atoms) in the center.[58]

Amino acid modifications within the chromophore core tend to drastically affect the color and photochemical aspects of GFP, specifically those at positions 65-67.[47] This region of the wild-type protein involves three covalently bonded amino acids, Ser-65, Tyr-66, and Gly-67; with the Tyr66 position being the most common to modify through introduction of an unnatural amino acid (Scheme 4.1).[59]

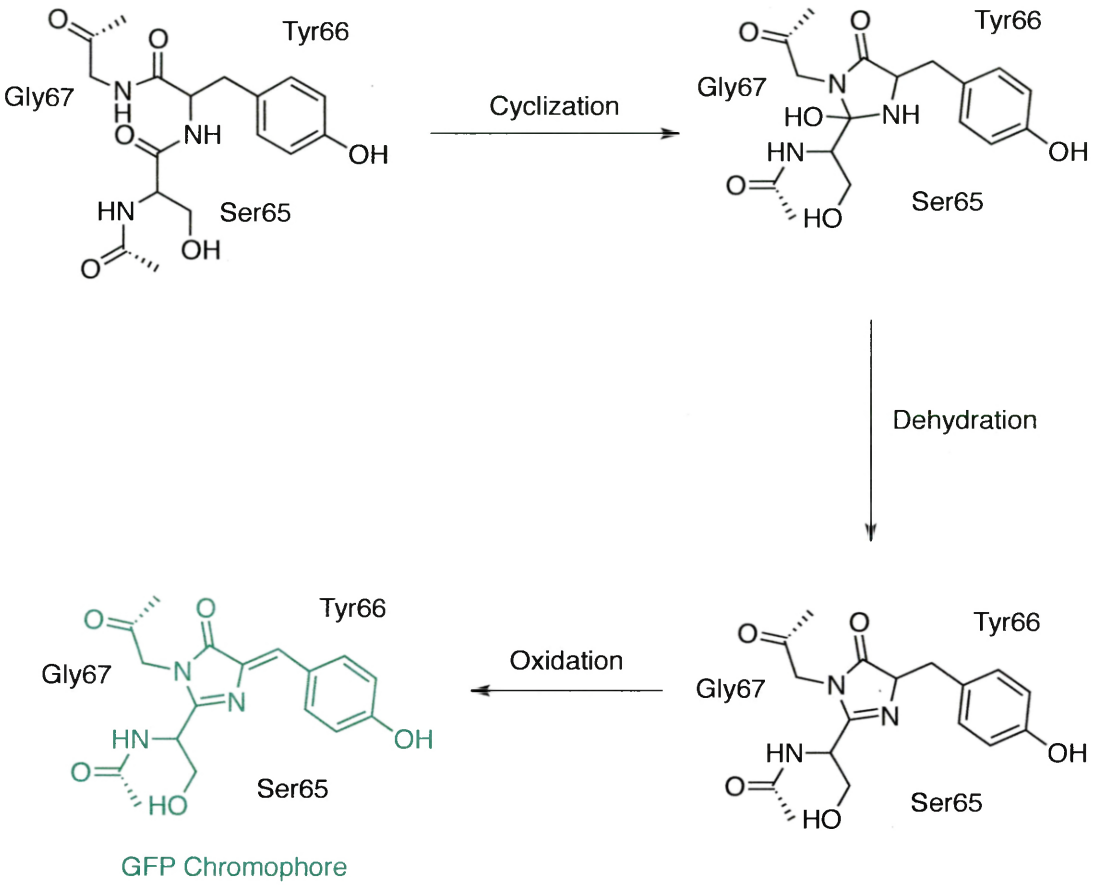

Scheme 4.1 –Steps to form cyclized chromophore within GFP.[59]

Our work investigated the addition of various fluorinated tyrosine derivatives into the chromophore core due to the electronegative effects of fluorine. The electronegativity of fluorine may alter the wavelengths of the absorbed and emitted light from the protein because it will alter electronic nature of the chromophore. By adding multiple fluorine substituents in numerous locations, we sought to establish a diverse series of proteins with a diverse range of pK_as (Figure 4.5). Further fluorescence analysis would reveal the impact that these substituents have on the physical properties of the modified GFP. Thankfully, the Schultz lab had previously evolved an aminoacyl-tRNA synthetase

(aaRS) designated for the incorporation of 2,3,5-trifluortyrosine into bacterial cells.[60]

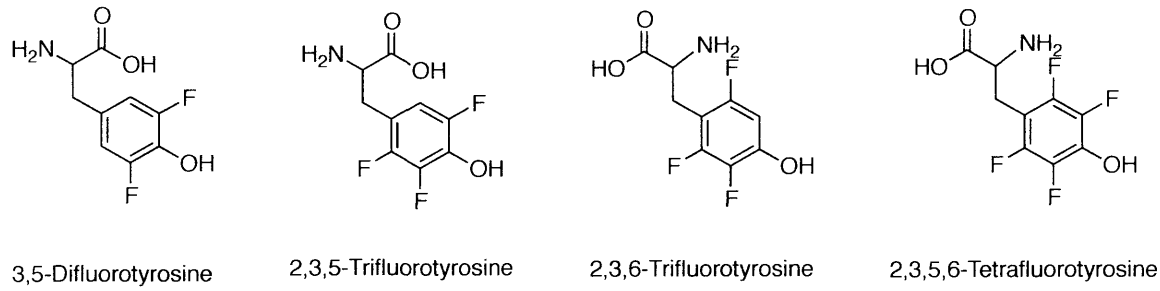

Figure 4.5 –Series of fluorinated unnatural tyrosine derivatives.

We attempted to express a variety of GFP derivatives containing one of the unnatural fluorinated amino acids and they were then analyzed for fluorescent properties by the Harbon lab. The presence of the various fluorine groups alters the pK_a of the tyrosine phenol, giving rise to different fluorescence properties depending on whether the phenol is protonated or deprotonated. Ultimately, these different GFP species could be utilized as biosensors fused to target proteins. Each unnatural amino acid has a unique pK_a, which would respond to pH changes in the environment. In this way multiple proteins within the same system could be traced by simply varying the wavelength of light used in the visualization process.

4.2 Results

4.2.1 Incorporation of Fluorotyrosine Derivatives

In order to generate a set of GFP targets for fluorescence analysis, we first obtained the fluorinated unnatural amino acids. By transforming cells with the previously

designed fluorotyrosine tRNA synthetase (3-FY aaRS) as well as with a plasmid coding for GFP with a TAG codon at position 66, we established the translational machinery necessary for the desired site-specific incorporation. After the transformation, cells were plated and grown in media containing both ampicillin and chloramphenicol antibiotics. This ensured that the cells continued to harbor both plasmids. Furthermore, the presence of the antibiotics deterred the growth of other species of bacteria or strains of *E. coli* that did not harbor the desired plasmid. Once the required translational machinery was established, cell cultures were grown to OD_{600} of 0.6-0.8 prior to induction of protein expression. Each induction involved the addition of isopropyl ß-D-1-thiogalactopyranoside (IPTG), arabinose, and the desired unnatural amino acid to the growth media. After the induced cells were grown at 30 °C for 16 h, the cells were pelleted and lysed. Due to the hexa-histidine tag on the GFP protein, the lysate was purified through a nickel spin column kit in order to isolate the GFP containing an unnatural amino acid. This method was successfully employed to generate proteins with 3,5-difluorotyrosine, 2,3,5-trifluorotyrosine, or 2,3,6-trifluorotyrosine in response to the TAG codon at position 66.

Unfortunately the 2,3,5,6-tetrafluorotyrosine amino acid was impermeable to the cell wall and thus could not be incorporated into the position 66 of the GFP. The presence of all four fluorine atoms dramatically reduced the pK_a of the hydroxyl group of the molecule through inductive effects. By pulling electron density away from the hydroxyl proton, the fluorine substituents lead to the deprotonation of the phenol within the growth media. In order to address this issue, we proposed linking the fluorotyrosine amino acid to another amino acid that would help transport it into the cell for incorporation. An

alanine amino acid was chosen for the formation of this dipeptide, due to its relatively inert effects on the system as well as its hydrophobic nature. Ideally, once the dipeptide successfully diffused across the cellular wall, various proteases could cleave the amide bond of the dipeptide. At this stage, the translational machinery can utilize the unnatural amino acid, with the ribosome inserting it into GFP.

In order to synthesize the dipeptide of interest, we coupled the protected amino acids in the presence of 1-ethyl-3-(3-dimethylaminopropyl)carbodiimide (EDCI) (Scheme 4.2).

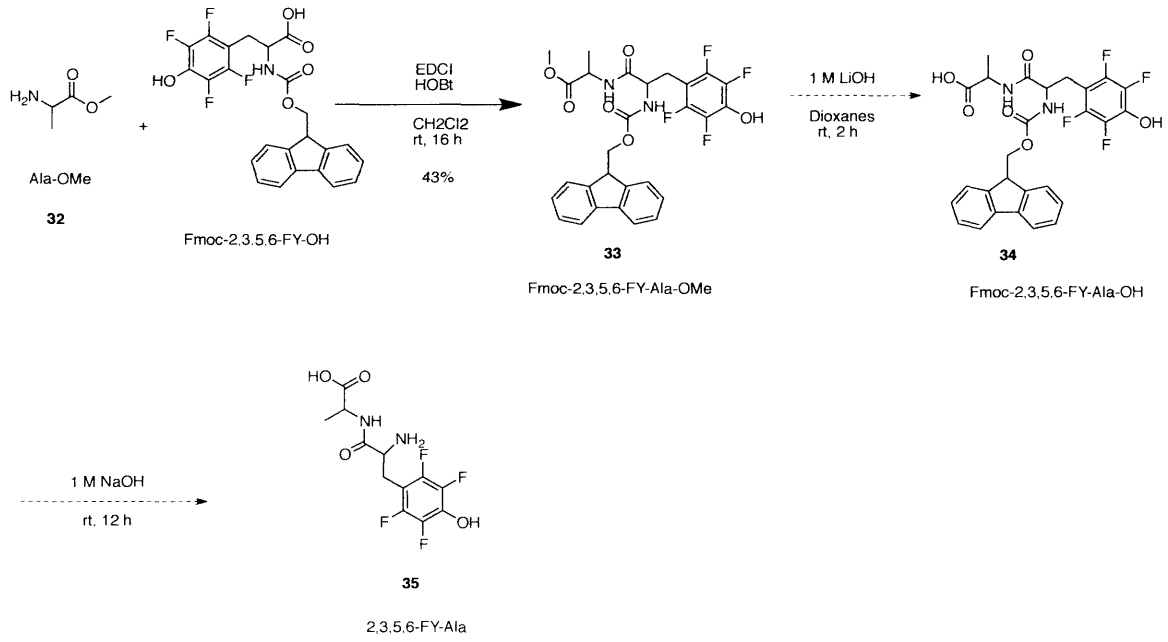

Scheme 4.2 – Synthesis of the 2,3,5,6-FY-Ala dipeptide.

After further purification, we removed the methoxy-protecting group from the molecule in 1 M LiOH at room temperature. Unfortunately, the removal of the Fmoc protecting group proved more difficult and was not confirmed by ^{1}H NMR. Future work

in this area centers on successfully removing the Fmoc protecting group before attempting to express this unnsatural amino acid in GFP. Without the removal of the Fmoc group, the ribosome will be unable to utilize the amino acid in forming peptide chains or proteins.

4.2.2 Syntheses of 2-amino-5-mercaptopentanoic acid and 2-amino-5-hydroxypentanoic acid Unnatural Amino Acids

In a separate collaboration with the Poutsma lab, we decided to synthesize a variety of unnatural amino acids, with varying methylene chains, including 2-amino-5-mercaptopentanoic acid **36** and 2-amino-5-hydroxypentanoic acid **37** (Figure 4.6). Once synthesized, the Poutsma lab utilized gas phase ion chemistry techniques in order to investigate the acid and base properties for these molecules.

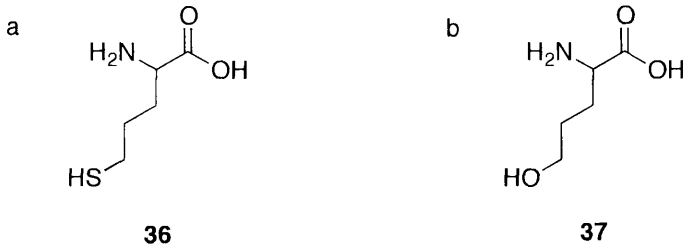

36 **37**

Figure 4.6 – (a) The chemical structures of the 2-amino-5-mercaptopentanoic acid, or homohomocysteine, and (b) 2-amino-5-hydroxypentanoic acid or homohomoserine unnatural amino acids.

In order to prepare **36**, the disulfide dimer had to be reduced. To achieve complete reduction of the undesired disulfide bonds, the sample was reacted with an excess of dithiothreitol (DTT) for 16 h (Scheme 4.3).

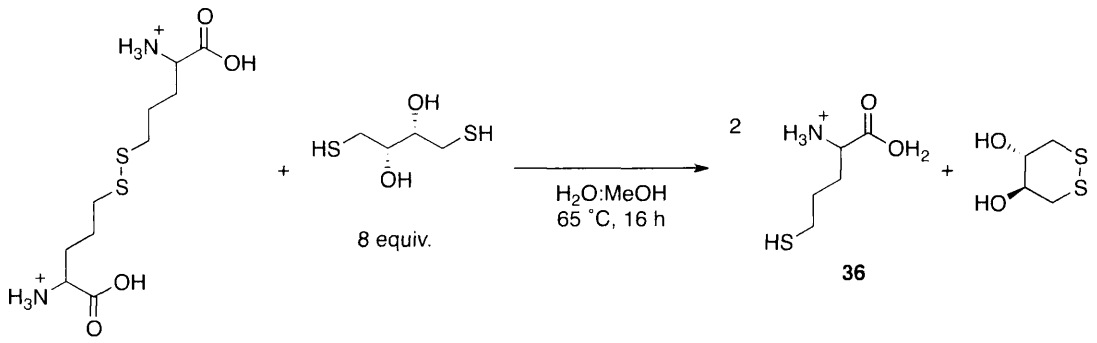

Scheme 4.3 – Reduction of 2-amino-5-mercaptopentanoic acid disulfide bonds.

After the removal of solvent *in vacuo*, the sample was resuspended to a concentration of ~10^{-2} M in a 1:1 methanol/water solution. The unnatural amino acid **36** was further analyzed by mass spectrometry by the Poutsma lab.

The 2-amino-5-hydroxypentanoic acid was synthesized based on previous literature precedent.[61] This method involved the reduction of a glutamate analog with lithium borohydride, an ester reducing agent (Scheme 4.4).

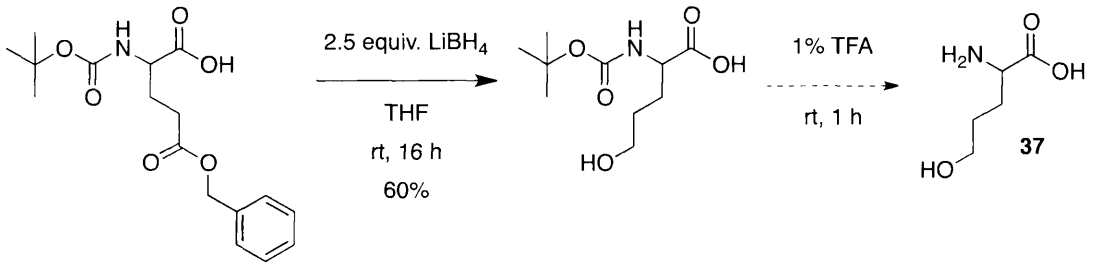

Scheme 4.4 – Selective reduction of ester functionality by lithium borohydride.

After reduction of the Boc-Glu(Obzl)-OH starting material, the remaining solvent was removed *in vacuo* and the product was confirmed by ^{1}H and ^{13}C NMR to verify the

reduction of the carbonyl carbon to the corresponding methylene. Future work involves removal of the protecting group by stirring in 1% TFA at room temperature for 1 h followed by removal of the solvent. The final product will be dissolved in 1:1 methanol/water for a final concentration of $\sim 10^{-2}$ M in a 1:1 methanol/water solution then given to the Poutsma lab for further analysis with the mass spectrometer. Future work on this project requires the deprotection of the 2-amino-5-hydroxypentanoic acid compound in TFA, before it is subjected to further analysis.

4.3 Materials and Methods

General. Solvents and reagents were obtained from either Sigma-Aldrich or Fisher Scientific and used without further purification, unless noted. Reactions were conducted under ambient atmosphere with un-distilled solvents, unless otherwise noted. NMR data was acquired on a Varian Gemini 400 MHz. *Escherichia coli* BL21(DE3) cell lines were obtained from Novagen. The various plasmids utilized during the transformations were obtained through either collaborators or Novagen.

Expression of GFP with Insertion of Fluorotyrosine Derivatives

A pET-GFPTAG66 plasmid and a pEVOL-3FY plasmid (0.5 μL each) were added to competent BL21(DE3) cells (50 μL; Novagen). The cells were transformed using electroporation techniques (1.8 V, 1s), then recovered in 2xYT media (500 μL) at 37 °C for 1 h. After plating on an LB agar containing ampicillin (50 μg/mL) and chloramphenicol (50 μg/mL), the cells were incubated overnight. A single colony was then used to inoculate 2xYT containing ampicillin (50 μg/mL) and chloramphenicol (50

μg/mL) (4 mL). After an overnight incubation at 37 °C, the starter culture (700 μL) was used to inoculate 2xYT media containing ampicillin and chloramphenicol (10 mL ea.). These expression cultures were incubated with shaking at 37 °C until the OD_{600} reached 0.7. At this point, one of the expression cultures was induced with 1M IPTG (10 μL) and 20% arabinose (10 μL). The other culture was induced with 1M IPTG (10 μL) and 20% arabinose then 100mM fluorinated tyrosine derivative (100 μL) was added. The cultures were then grown for 16 hours at 30°C. Both expression cultures were pelleted at 4000 rpm for 20 minutes, and then frozen at -80 °C for 20 minutes. The cell pellets were resuspended in Bug Buster (500 μL; Novagen) supplemented with lysozyme to lyse the cells. The cell mixture was incubated at room temperature for 20 minutes, and then centrifuged at 13,000 rpm for 20 minutes. The supernatant was then added from the QIAGEN® Ni-NTA Spin Column, and the resulting proteins were purified according to the manufacturer's protocols. GFP expression was assessed by fluorescence analysis in the Harbron Lab.

Synthesis of 2,3,5,6-Fluorotyrosine-Alanine Dipeptide

Preparation of Alanine Amino Acid

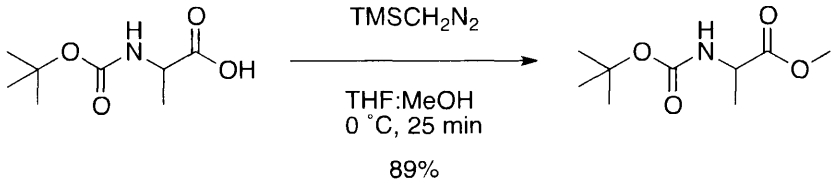

Boc-Ala-OH was added to a flame-dried vial (500 mg, 2.6 mmol, 1 equiv.) equipped with a stir bar then dissolved in a THF:MeOH solvent (9 mL: 4.5mL). The solution was cooled in an ice bath to 0 °C for 25 min, then $TMSCH_2N_2$ in hexanes (2.6 mL, 2.0 M, 5.2

mmol) was added dropwise over 10 min. The mixture was stirred at 0 °C for an additional 20 min. The solvent was evaporated *in vacuo,* and the resin was purified by silica gel flash chromatography (Hexane:Ethyl Acetate, 3:1) to give a clear oil (470 mg, 2.3 mmol, 89%). **Boc-Ala-OMe:** ^{1}H NMR (400 MHz; $CDCl_3$): ∂ 4.23-4.19 (m, 1H), 3.62 (s, 3H), 1.37 (s, 9H), 1.28 (d, J = 6.9 Hz, 3H).

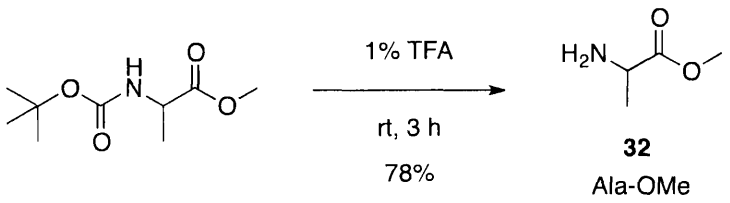

The Boc-Ala-OMe product (470 mg, 2.3 mmol) was dissolved in 1% TFA in CH_2Cl_2 (5 mL) then stirred at rt for 3 h. After removal of the solvent *in vacuo* a clear oil remained (390 mg, 1.80 mmol, 78%). **H-Ala-OMe (32):** ^{1}H NMR (400 MHz; CD_3OD) ∂ 8.45 (s, 1H), 4.12 (q, J = 6.8 Hz, 1H), 3.79 (s, 3H), 1.48 (d, J = 6.8 Hz, 3H).

Dipeptide Coupling Reaction

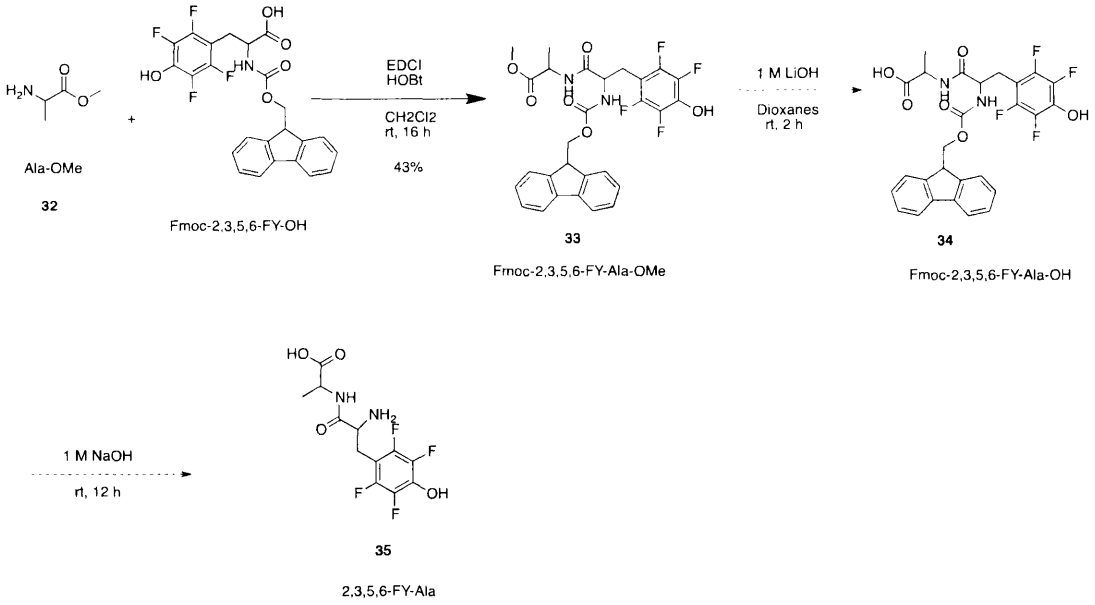

Fmoc-2,3,5,6-tetrafluoridetyrosine-OH (25 mg, 0.05 mmol, 1 equiv.), H-Ala-OMe (5 mg, 0.05 mmol, 1 equiv.), triethylamine (7 μL, 0.05 mmol, 1 equiv.), and hydroxybenzotriazole (HOBt; 7 mg, 0.05 mmol, 1 equiv.) were added to a flame dried vial equipped with a stir bar. The solution was dissolved in 5% DMF/DCM (2 mL) then 1-Ethyl-3-(3-dimethylaminopropyl)carbodiimide (EDCI; 10 mg, 0.053, 1.05 equiv.) was added in portions over 5 min. The reaction was stirred at rt for 24 h, then washed with brine. The product was extracted in DCM (3 x 5 mL), dried with magnesium sulfate then filtered. The solvent was evaporated *in vacuo,* and the resin was purified by silica gel flash chromatography (Hexane:Ethyl Acetate, 4:1) to give a white solid (13 mg, 0.02 mmol, 43%). **Fmoc-2,3,5,6-FY-Ala-OMe (33):** ^{1}H NMR (400 MHz; $CDCl_3$): ∂ 7.78 (d, J = 7.5 Hz, 2H), 7.57 (d, J = 1.5 Hz, 2H), 7.38 (t, J = 7.5 Hz, 2H), 7.29 (t, J = 7.4 Hz, 2 H), 4.62 (t, J = 6.9 Hz, 1H), 4.52 (d, J = 6.8 Hz, 2H), 4.36 (t, J = 6.9 Hz, 1H), 4.25 (t, J = 7.0 Hz, 1H), 3.69 (s, 3H), 3.22-3.05 (m, 2H), 1.38 (d, J = 6.8 Hz, 3H).

The Fmoc-2,3,5,6-FY-Ala-OMe was dissolved in dioxanes (500μL) then chilled to 0 °C for 10 min. Lithium hydroxide (LiOH; 500 μL, 1 M) was slowly added to the reaction then the solution was warmed to room temperature. The reaction was stirred at room temperature for 1 h then acidified at 0 °C with HCl (1M). After an extraction in ethyl acetate (3 x 5 mL) the solvent was removed *in vacuo.*

Reduction of 2-amino-5-mercaptopentanoic acid (36)

The disulfide bonded 2-amino-5-mercaptopentanoic acid dimer (15 mg, 0.050 mmol, 1 equiv.) was added to a vial then dissolved in 1:1 H_2O/MeOH (2.5 mL each.). Dithiothreitol (DTT; 65 mg, 0.421 mmol, 8 equiv.) was added to the stirring reaction then the reaction was stirred at 65 °C for 16h. The Poutsma lab confirmed complete reduction of the disulfide bonds by injecting the sample into the triple quadrupole MS.

Synthesis of 2-amino-5-hydroxypentanoic acid (37)

Boc-Glu(OBzl) (200 mg, 0.59 mmol, 1 equiv.) was dissolved in anhydrous THF (1.0 mL), and then $LiBH_4$ (31.5 mg, 1.45 mmol, 2.5 equiv.) was added to the solution with stirring at room temperature under argon for a further 16 h. Ethyl acetate (1.0 mL) was added, and the solution was stirred at room temperature for 3 h. After evaporation, the reaction mixture was subjected to silica gel column chromatography (10:1 CH_2Cl_2:MeOH). After removal of the solvent *in vacuo* a white solid remained (83 mg, 0.36 mmol, 60%). **Boc-2-amino-5-hydroxypentanoic acid (37):** ^{1}H NMR (400 MHz; $CDCl_3$): ∂ 8.70 (s, 1H), 4.62 (q, J = 6.8 Hz, 1H), 3.62 (s, 3H), 1.68 (d, J = 6.8 Hz, 3H).

REFERENCES

1. Gedye, R; Smith, F.; Westway, K.; Ali, H.; Baldisera, L.; Laberge, L.; Rousell, R. The Use of Microwave Ovens for Rapid Organic Synthesis. *Tetrahedron Letters* **1986**, 27, 279-282.

2. Giguere, R. J.; Bray, T. L.; Duncan, S. M.; Majetich, G. Application of Commercial Microwave Ovens to Organic Synthesis. *Tetrahedron Letters* **1986**, 27, 4945–4948.

3. Polshettiwar, V.; Varma, R. S. Aqueous Microwave Chemistry: A Clean and Green Synthetic Tool for Rapid Drug Discovery. *Chemical Society Reviews* **2008**, 37, 1546–1557.

4. Kappe, C. O.; Dallinger, D. The Impact of Microwave Synthesis on Drug Discovery. Nature Reviews Drug Discovery 2006, 5, 51–63.

5. Pedersen, S. L.; Tofteng, A. P.; Malik, L.; Jensen, K. J. Microwave Heating in Solid-Phase Peptide Synthesis. *Chemical Society Reviews* **2012**, 41, 1826–1844.

6. Klinowski, J.; Paz, F. A. A.; Silva, P.; Rocha, J. Microwave-assisted Synthesis of Metal-organic Frameworks. *Dalton Transactions* **2011**, 40, 321–330.

7. Electro Magnetic Spectrum. http://zebu.uoregon.edu/~imamura/122/images/electromagnetic-spectrum.jpg (Accessed July 3, 2103).

8. Kappe, C.O. Controlled Microwave Heating in Modern Organic Synthesis. *Angewandte Chemie International Edition* **2004**, 43, 6250-6284.

9. Lidstroèm, P.; Tierney, J.; Wathey, B.; Westman, J. Microwave Assisted Organic Synthesis - A Review. *Tetrahedron* **2001**, 57, 9225-9283.

10. Leadbeater, N.E.; Marco, M. Ligand-Free Palladium Catalysis of the Suzuki Reaction in Water Using Microwave Heating. *Organic Letters* **2002**, 4, 2973 – 2976.

11. Appukkuttan, P.; Dehaen, W.; Fokin, V.V.; Van der Eycken, E.A Microwave-Assisted Click Chemistry Synthesis of 1,4-Disubstituted 1,2,3-Triazoles via a Copper(I)-Catalyzed Three-Component Reaction. *Organic Letters* **2004**, 6, 4223-4225.

12. Stadler, A.; Yousefi, B.H.; Dallinger, D.; Walla, P.; Van der Eycken, E.; Kaval, N.; Kappe, C.O. Scalability of Microwave-Assisted Organic Synthesis. From Single-Mode to Multimode Parallel Batch Reactors. *Organic Process Research & Development* **2003**, 7, 707 – 716.

13. Williams, L. Thin layer chromatography as a tool for reaction optimization in microwave assisted synthesis. *Chemical Communications* **2000**, 6, 435-436.

14. Van der Eycken, E.; Appukkuttan, P.; De Borggraeve, W.; Dehaen, W.; Dallinger, D.; Kappe, C.O. High-Speed Microwave-Promoted Hetero-Diels–Alder Reactions of 2(1*H*)-Pyrazinones in Ionic Liquid Doped Solvents. *The Journal of Organic Chemistry* **2002**, 67, 7904-7907.

15. Dandepally, S.R.; Williams, A.L. Microwave-assisted N-Boc deprotection under mild basic conditions using $K_3PO_4 \cdot H_2O$ in MeOH. *Tetrahedron Letters* **2009**, 50, 1071-1074.

16. Shi Shun, A.L.; Tykwinski, R.R.Synthesis of Naturally Occurring Polyynes. *Angewandte Chemie International Edition* **2006**, 45, 1034-1057.

17. Wong, W.Y.; Long, N.J.; Williams, C.K. Recent Advances in Luminescent Transition Metal Polyyne Polymers. *Angewandte Chemie International Edition* **2003**, 42, 2586.

18. Klebansky, A.L.; Grachev, I.V. Kuznetsova, O.M. *Russian Journal of General Chemistry* **1957**, 27, 3008-3013.

19. Bohlmann, F.; Schonowsky, H.; Inhoffen, E.; Grau, G. Polyacetylenverbindungen, LII. Über den Mechanismus der oxydativen Dimerisierung von Acetylenverbindungen. Chemische Berichte **1964**, 97, 794-800.

20. Siemsen, P.; Livingston, R.C; Diederich, F. Acetylenic Coupling: A Powerful Tool in Molecular Construction. *Angewandte Chemie International Edition* **2000**, 39, 2632-2657.

21. Villhelmsen, M.H.; Jensen, J.; Tortzen, C.G.; Nielsen, M.B. The Glaser–Hay Reaction: Optimization and Scope Based on ^{13}C NMR Kinetics Experiments. *European Journal of Organic Chemistry* **2013**, 2013, 701-711.

22. Chodkiewicz, W.; Cadiot, P. *Annales des Chimie.* **1957**, 2, 819-869.

23. Lu, W.; Zheng, G.; Aisa, H.A.; Cai. J. First total synthesis of optically active panaxydol, a potential antitumor agent isolated from Panax ginseng. . *Tetrahedron Letters* **1998**, 39, 9521-9522.

24. Zhang, H.C.; Brumfield, K. K.; Jaroskova, L.; Maryanoff, B. E. Facile substitution of resin-bound indoles via the Mannich reaction. *Tetrahedron Letters* **1998**, *39*, 4449-52.

25. Larhed, M.; Lindeberg, G.; Hallberg, A. Rapid Microwave-Assisted Suzuki Coupling on Solid-Phase. *Tetrahedron Letters* **1996**, 37, 8219-8222.

26. Franzén, R. The Suzuki, the Heck, and the Stille reaction — three versatile methods for the introduction of new C—C bonds on solid support. *Canadian Journal of Chemistry* **2000**, 78, 957-962.

27. Tierney,S.; Heeney, M.; McCulloch, I. Microwave-assisted synthesis of polythiophenes via the Stille coupling. *Synthetic Metals* **2005**, 148, 195-198.

28. Li, L.; Wang, J.; Liu, Q. A mild copper-mediated Glaser-type coupling reaction under the novel CuI/NBS/DIPEA promoting system. *Tetrahedron Letters* **2009**, 50, 4033-4036.

29. Bhandari, M.R.; Yousufuddin, M.; Lovely, C.J. Diversity-Oriented Approach to Pyrrole-Imidazole Alkaloid Frameworks. *Organic Letters* **2011**, 13, 1382–1385.

30. About Biotech. http://www.accessexcellence.org/RC/AB/WYW/cohen/cohen_4.php (Accessed June 30, 2103).

31. Edwards, W.F.; Young, D.D.; Deiters, A. The effect of microwave irradiation on DNA hybridization. *Organic & Biomolecular Chemistry* **2009**, 7, 2506-2508.

32. Fermér, C.; Nilsson, P.; Larhed, M. Microwave-assisted high-speed PCR. *European Journal of Pharmaceutical Sciences* **2003**, 2, 129-132.

33. Parker, M.C.; Besson, T.; Lamare, S.; Legoy, M.D. Microwave Radiation Can Increase The Rate of Enzyme-Catalysed Reactions in Organic Media. *Tetrahedron Letters* **1996**, 37, 8383-8386.

34. Fregel, R.; Rodríguez, V.; Cabrera, V.M. Microwave improved Escherichia coli transformation. *Letters in Applied Microbiology* **2008**, 46, 489-499.

35. CoolMate – Sub-ambient Synthesis. http://www.cem.com/e107_images/custom/ColMte_Anim.gif (Accessed June 28, 2013).

36. Tripp, V.T.; Maza, J.C.; Young, D.D. Development of rapid microwave-mediated and low-temperature bacterial transformations. *Journal of Chemical Biology* **2013**, 6, 135-140.

37. Dityatkin S.Y.; Lisovskaya, K.V.; Panzhava, N.N.; Iliashenko, B.N. Frozen-thawed bacteria as recipients of isolated coliphage DNA. *Biochimica et Biophysica Acta* **1972**, 281, 319-323.

38. Wise, A.A.; Liu, Z.; Binns, A.N. Three methods for the introduction of foreign DNA into Agrobacterium. *Methods in Molecular Biology* **2006**, 343, 43-53.

39. Weigel, D.; Glazebrook, J. Transformation of Agrobacterium using the freeze-thaw method. *CSH Protoc* **2006**, 2006(7).

40. Takahashi, R.; Valeika, S.R.; Glass, K.W. A simple method of plasmid transformation of E. coli by rapid freezing. *Biotechniques* **1992**, 13, 711-715.

41. Chen, H.; Nelson, R.S.; Sherwood, J.L. Enhanced recovery of transformants of Agrobacterium tumefaciens after freeze-thaw transformation and drug selection. *Biotechniques* **1994**,16, 664–668.

42. Shokolenko, I.N.; Alexeyev, M.F. Transformation of Escherichia coli TG1 and Klebsiella oxytoca VN13 by freezing- thawing procedure. *Biotechniques* **1995**, 18, 596-598.

43. Hanahan, D. Studies on transformation of *Escherichia coli* with plasmids. *Journal of Molecular Biology* **1983**, 166, 557-580.

44. Wards, B.; Collins, D. Electroporation at elevated temperatures substantially improves transformation efficiency of slow- growing mycobacteria. *FEMS Microbiology Letters* **1996**, 145, 101-105.

45. Daugelat, S.; Kowall, J.; Mattow, J.; Bumann, D.; Hurwitz, R.; Kaufmann, S.H. The RD1 proteins of Mycobacterium tuberculosis: expression in Mycobacterium smegmatis and biochemical characterization. *Microbes and Infection* **2003**, 12, 1082.1095.

46. Wang, L.; Brock, A.; Herberich, B.; Schultz, P.G. Expanding the Genetic Code of *Escherichia coli*. *Science* **2001**, 292, 498-500.

47. Kowal, A.K.; Köhrer, C.; RajBhandary, U.L. Twenty-first aminoacyl-tRNA synthetase-suppressor tRNA pairs for possible use in site-specific incorporation of amino acid analogues into proteins in eukaryotes in eubacteria. *Proceedings of the national Academey of Sciences of the United States of America* **2001**, 98, 2268-2273.

48. Jackson, J.C.; Duffy, S.P.; Hess, K.R.; Mehl, R.A. Improving Nature's Enzyme Active Site with Genetically Encoded Unnatural Amino Acids. *Journal of the American Chemical Society* **2006**, 128, 11124-11127.

49. Kiick, K.L.; Saxon, E.; Tirrell, D.A.; Bertozzi, C.R. Incorporation of azides into recombinant proteins for chemicselective modification by the Staudinger ligation. *Proceedings of the national Academey of Sciences of the United States of America* **2002**, 99, 19-24.

50. Wang, J.; Xie, J.; Schultz, P.G. A Genetically Encoded Fluorescent Amino Acid. *Journal of American Chemical Society* **2006**, 128, 8738-8739.

51. Novoa, E.M.; Ribas de Pouplana, L. Speeding with control: codon usage, tRNAs, and ribosomes. *Trends in Genetics* **2012**, 28, 574-581.

52. Function and Role of tRNA Synthetases http://www.cs.stedwards.edu/chem/Chemistry/CHEM43/CHEM43/tRNA/Function.htm (Accessed on June 28, 2013).

53. tRNA. http://www.wiley.com/college/boyer/0470003790/structure/tRNA/trna_intro.htm (Accessed on June 28, 2013).

54. Gustilo, E.M.; Vendeix. F.A.; Agris, P.F. tRNA's modifications bring order to gene expression. *Current Opinion in Microbiology* **2008**, 11, 134–140.

55. Liu, C.C.; Schultz, P.G. Adding new chemistries to the genetic code. *Annual Review of Biochemistry* **2010**, 79, 413-444.

56. Wang: Research Group Site. http://wang.salk.edu/research.php (Accessed July 3, 2013).

57. Wang, L., Xie, J., Ashok, D.A., & Schultz, P.G. Unnatural Amino Acid Mutagenesis of Green Fluorescent Protein. *The Journal of Organic Chemistry* **2003**, 68, 174-176.

58. Green Fluorescent Protein: Protein Data Bank. http://www.wwpdb.org (Accessed on June 28, 2013).

59. Reid, B.G.; Flynn, G.C. Chromophore Formation in Green Fluorescent Protein. *Biochemistry* **1997**, 36, 6786-6791.

60. Minnihan, E.C.; Young, D.D.; Schultz, P.G.; Stubbe, J. Incorporation of fluorotyrosines into ribonucleotide reductase using an evolved, polyspecific aminoacyl-tRNA synthetase. *The Journal of American Chemical Society* 2011, *40*, 15942-15945.

61. Kisugi, T.; Okino, T. Micropeptins from the Freshwater Cyanobacterium *Microcystis aeruginosa* (NIES-100). *Journal of Natural Products* **2009**, 72, 777–781.